

THE DEZINCIFICATION OF ALPHA AND BETA BRASSES

By

Robert Henry Heidersbach, Jr.

A Dissertation Presented to the Graduate Council
of the University of Florida
in Partial Fulfillment of the Requirements for the
Degree of Doctor of Philosophy

UNIVERSITY OF FLORIDA

DECEMBER, 1971

Dedicated to my wife, Dianne Katherine.

ACKNOWLEDGEMENTS

I would like to express my thanks to Dr. Ellis D. Verink, Jr., for his guidance and inspiration. Thanks are also extended to the members of my committee, Dr. A. D. Wallace, Dr. R. T. DelHoff, Dr. R. W. Gould and Dr. J. J. Hren.

Dr. M. Pourbaix provided encouragement during the early stages of this investigation. Dr. S. R. Bates provided guidance on the use of and interpretation of results from the scanning electron microscope and the electron microprobe. Mr. W. C. Fort III, provided invaluable assistance in obtaining the experimental results. Technical assistance was provided by Mr. W. A. Acree, Mr. E. J. Jenkins, Mr. E. C. Logsdon, Mr. P. D. Kalb, Mr. C. J. Minier and Mr. C. Simmons.

I particularly wish to acknowledge the financial support supplied by the National Association of Corrosion Engineers and by the International Nickel Company. In addition, certain of the equipment used in the electrochemical studies was purchased with funds from the Office of Saline Water.

The Chase Brass and Copper Company donated the alpha brass used in this investigation, and this contribution is gratefully acknowledged.

The author is grateful to his parents, who taught him the dignity of hard work, and to his wife, who made life bearable when things were not going according to plans.

TABLE OF CONTENTS

	Page
ACKNOWLEDGEMENTS	iii
LIST OF TABLES	vii
LIST OF FIGURES	viii
ABSTRACT	xi
INTRODUCTION	1
EXPERIMENTAL PROCEDURE	5
Immersion Test Apparatus	6
Electrochemical Test Apparatus	9
Sample Preparation	15
X-RAY DIFFRACTION	18
Present Work	24
ELECTRON MICROPROBE	30
Present Work	32
OPTICAL METHODS	41
Present Work	45
SOLUTION ANALYSIS	54
Present Work	58
ELECTROCHEMICAL INVESTIGATIONS	83
Present Work	88
DISCUSSION	105
CONCLUSIONS	116
RECOMMENDATIONS FOR FURTHER RESEARCH	119

TABLE OF CONTENTS (Continued)

	Page
APPENDIX	
1 EQUIPMENT USED IN ELECTROCHEMICAL TESTS	122
2 ELECTROLYTES	123
3 CHEMICAL ANALYSES OF ALPHA BRASS	125
4 BETA BRASS INGOT PREPARATION	127
5 PROCEDURE FOR THE ELECTROGRAVIMETRIC CHEMICAL ANALYSIS OF BINARY COPPER-ZINC ALLOYS	129
6 ANALYSIS OF BETA BRASS INGOTS USED IN THIS INVESTIGATION	131
7 ELECTROCHEMICAL SAMPLE PREPARATION	132
8 EQUATIONS USED IN CONSTRUCTION OF POTENTIAL VERSUS pH DIAGRAMS FOR THE Cu-Cl-H ₂ O SYSTEM AND THE ZnO-H ₂ O SYSTEM	133
BIBLIOGRAPHY	137
BIOGRAPHICAL SKETCH	145

LIST OF TABLES

Table		Page
1	Sample 6-19, Weight Information	53
2	Atomic Absorption Data for Alpha Brass in 5N HCl at 90.35°C	60
3	Atomic Absorption Data for Alpha Brass in 5N HCl at 98.50°C	61
4	Atomic Absorption Data for Beta Brass in 5N HCl at 59.60°C	62
5	Atomic Absorption Data for Beta Brass in 5N HCl at 67.50°C	63
6	Atomic Absorption Data for Beta Brass in 5N HCl at 89.35°C	64
7	Atomic Absorption Data for Beta Brass in 5N HCl at 99.85°C	66
8	Alpha Brass Potentiostatic Test Data	96
9	Beta Brass Potentiostatic Test Data	98
10	Alpha Brass Free Corrosion Potential Tests	102
11	Beta Brass Free Corrosion Potential Tests	103
12	Approximate Copper and Zinc Concentrations in Solutions Where Copper Deposits Were Observed on Alpha Brass	109

LIST OF FIGURES

Figure		Page
1	Immersion test cell	7
2	Circuit diagram of equipment used to polarize specimen and automatically record corrosion current density as a function of potential	10
3	Corrosion cell used in electrochemical investigations	11
4	Assembled and exploded views of sample holder	13
5	Copper-zinc phase diagram	19
6	Copper-gold phase diagram	20
7	The lattice parameter of alpha brass as a function of the atomic percent zinc	22
8	(111) peaks of a mixture of 70-30 brass filings and copper filings	25
9	(111) peaks from sample of 70-30 brass dezincified for 20 days in 5N HCl at 75°C	26
10	(111) peaks from sample of 70-30 brass dezincified for 30 days in 5N HCl at 75°C	27
11	Diffraction pattern from sample of beta brass dezincified for two days in 5N HCl at 75°C	29
12	Zinc intensity profile from a sample of alpha brass dezincified for 79 days in 1N NaCl	34
13	Zinc intensity profile from a sample of alpha brass dezincified for 10 days in 5N HCl at 75°C	35

LIST OF FIGURES (Continued)

Figure		Page
14	Zinc intensity profile from a sample of beta brass dezincified for two days in 5N HCl at 75°C	36
15	Photomicrograph of sample shown in Figure 12	38
16	Photomicrograph of sample shown in Figure 13	39
17	Photomicrograph of sample shown in Figure 14	40
18	Dezincification plug in 70-30 alpha brass exposed for 79 days in 1N NaCl at room temperature	42
19	Copper deposits on the surface of dezincified alpha brass sample	47
20	Deposit on surface of dezincified alpha brass sample	48
21	Scanning electron micrograph of copper slab protruding from the surface of a dezincified alpha brass sample	49
22	Nondispersive x-ray analyzer pattern of deposit shown in Figure 21	51
23	Dezincified cross-section of sample shown in Figure 21	52
24	Atomic-absorption calibration curve for copper	68
25	Copper and zinc dissolution from alpha brass in 5N HCl at 90.35°C	71
26	Copper and zinc dissolution from alpha brass in 5N HCl at 98.50°C	72
27	Dezincification factors, Z, for alpha brass in 5N HCl at 98.50°C	73
28	Copper dissolution from beta brass in 5N HCl at 67.50°C	75

LIST OF FIGURES (Continued)

Figure		Page
29	Zinc dissolution from beta brass in 5N HCl at 67.50°C	76
30	Dezincification factors, Z, for beta brass in 5N HCl at 67.50°C	77
31	Zinc dissolution from beta brass in 5N HCl at various temperatures	78
32	Arrhenius plot of zinc dissolution rate versus 1000/T	80
33	Experimental potential versus pH diagram for 70 Cu - 30 Zn in 0.1M Cl ⁻ at 25°C	89
34	Simplified Cu-Cl-H ₂ O diagram at 25°C for solution containing 0.1M chloride ions	90
35	Simplified Zn-H ₂ O diagram for concentrations of ionic species = 10 ⁻⁶ M	91
36	70 Cu - 30 Zn alloy in 0.1M chloride solution	92
37	Beta brass held at +0.050V _{SHE} for 2-3/4 hours	94
38	Typical potentiokinetic scan in acid solutions	100
39	Cross-section of alpha brass showing where holidays in the stop-off lacquer caused de- zincification in the stagnant regions beneath the holidays	110
40	Theoretical domains for dealloying in a given solution based upon the Nernst equation	114

Abstract of Dissertation Presented to the Graduate Council
of the University of Florida in Partial Fulfillment of the
Requirements for the Degree of Doctor of Philosophy

THE DEZINCIFICATION OF ALPHA AND BETA BRASSES

By

Robert Henry Heidersbach, Jr.

December, 1971

Chairman: Dr. Ellis D. Verink, Jr.
Major Department: Metallurgical and Materials Engineering

The mechanisms of dezincification of single-phase alpha and beta brasses were studied using x-ray diffraction, electron microprobe, metallographic, atomic absorption, and electrochemical techniques.

The two mechanisms of dezincification which had been previously reported, (1) dissolution of both alloy constituents followed by redeposition of the more noble species, and (2) the selective removal of the less noble constituent, were found to be operative under certain conditions of potential and pH for both alpha and beta brasses.

An electrochemical explanation of the circumstances under which dealloying can be expected to occur was developed based on the use of Pourbaix diagrams.

INTRODUCTION

Dealloying is a corrosion process whereby one constituent of an alloy is preferentially removed from the alloy, leaving an altered residual structure.⁽¹⁾

While dezincification, the loss of zinc from brasses, is the most commonly experienced form of dealloying,⁽²⁻¹²⁾ other examples have been reported in practice. These include loss of nickel,^(2,13-15) aluminum^(9,16-22) and tin^(23,24) from copper alloys; iron from cast iron;⁽²⁵⁾ nickel from alloy steels⁽²⁶⁾ and cobalt from Stellite.⁽²⁷⁾

Since the phenomenon was first reported in 1866, the literature has been filled with reports of research efforts aimed at clarifying the mechanisms of dealloying. Nonetheless, there still is no general agreement as to the detailed mechanism involved. One group contends that the entire alloy is dissolved and that one of its constituents then is replated from solution.^(23,27-40) Another contends that one species is selectively dissolved from the alloy, leaving a porous residue of the more noble species.^(15,41-47) Still others believe that both mechanisms take place.^(16,48-54)

A number of literature surveys have appeared, and these summarize the situation up to the time they were written.^(1,49,55-58)

The study of dealloying phenomena is fraught with a number of complications. Generally, such reactions are relatively slow and a lengthy exposure period is required to cause a sufficiently great amount of dealloying to facilitate evaluation. Consequently, there is considerable interest in accelerated tests for evaluation of tendencies of alloys to dealloy. Many techniques have been employed. For example, electrolyte compositions have been adjusted by using more concentrated solutions or solutions having variations in oxidizing power.⁽⁵²⁾ Specific ions have been added to stimulate dealloying, e.g., saturated cuprous chloride solutions have been used to accelerate the dezincification of copper-base alloys.⁽⁴⁰⁾ Electrochemical stimulation also has been used. Unfortunately, all too often the test methods employed have been vulnerable to criticism as having biased the experimental result and, although specific techniques are now available which can cause dealloying to occur in the laboratory, nonetheless, there still is no firm basis for predicting the likelihood of dealloying in service based on these tests.

Single-phase alpha brasses and duplex alpha-plus-beta brasses are the only forms of copper-zinc alloys having engineering significance at present. Bengough and May reported, in 1922, that small additions of arsenic would prevent dezincification of alpha brasses but would not protect the beta phases of duplex alloys.⁽⁵⁹⁾ The reasons for

arsenic protecting alpha brass but not the beta phase of duplex alloys have remained controversial. (1,55,56) However, the addition of small amounts of arsenic, or of antimony or phosphorus, which have similar effects, has become a standard means of inhibiting dezincification in alpha brasses. (1) No inhibitor is presently available for duplex alloys, although the addition of tin retards most forms of brass corrosion to include dezincification. (1)

The purpose of this investigation has been to elucidate the mechanism of dezincification of alpha and of beta brasses and to develop a basis for predicting the conditions under which dezincification of these alloys might be expected to occur.

Particular emphasis was placed on selecting exposure conditions and test methods which would not bias the experimental results. For example, it was felt that accelerated tests using copper-chloride solutions could not give unbiased evidence for a dissolution-redeposition mechanism, although this method of accelerated testing has been reported frequently in the literature. (29,40,60-62) Electrochemical stimulation (in which the specimen was a driven anode) has also been used as a means of producing dezincification. (62-65) This method of producing accelerated attack also can bias the experimental results by masking the presence of diffusion-related selective-removal processes, because diffusion, as it is commonly understood, is a quite

slow process at the low temperatures encountered in aqueous environments.

Mechanism studies were performed on brass immersion samples placed in NaCl and HCl solutions. No copper salts were added to the test electrolyte except as the result of corrosion of the test specimens. Test durations of up to 90 days were employed at temperatures ranging from room temperature (approximately 25°C) to 100°C.

Potentiostatic and potentiokinetic methods were used to define conditions under which dealloying might be expected to occur.

EXPERIMENTAL PROCEDURE

The possibility of bias of results due to the testing method used was discussed in the introduction to this dissertation. Immersion testing of brass samples in environments known to produce dezincification was chosen as the laboratory test method most suited for a study of the mechanism of dealloying.

Electrochemical tests were employed in later stages of this investigation, after the mechanism studies were completed. These tests were intended to define the conditions of potential and pH under which particular modes of dealloying of copper-zinc alloys could be expected to occur.

Immersion Test Apparatus

Figure 1 is a diagram of the immersion test cell used in this investigation. It is similar in many respects to that recommended by National Association of Corrosion Engineers Standard TM-01-69, "Laboratory Corrosion Testing of Metals for the Process Industries."(66)

The cell is constructed of a Pyrex* glass resin reaction kettle held together by an external metal clamp. All fixtures inserted into the cell also are made of Pyrex, with the exception of the Teflon**-coated stirring bar.

Samples are suspended from a sample holder as shown in the diagram. In tests requiring an oxygen-free environment, liquid in the cell is sparged with dried and purified argon which enters the cell through a fritted-glass diffuser immersed in the liquid. Gas is passed out of the system by way of a Liebig-type reflux condenser which is backed up by a liquid trap to prevent solution loss or contamination. The volume of solution within the cell was measured at the start and finish of each test. Losses did not exceed 10 ml from an initial volume of 750 ml in tests of up to 30 days. This corresponds to a maximum change in solution volume of 1.3 percent. The normality of acids being used was also checked

*Registered trademark, Corning Glass Company.

**Registered trademark, E. I. duPont de Nemours and Company, Inc.

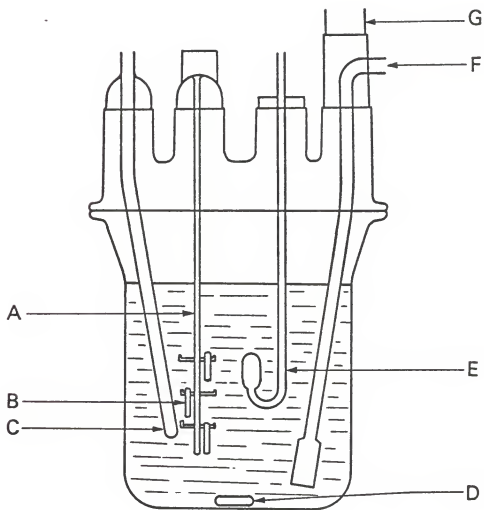


Figure 1. Immersion test cell. A - sample holder, B - sample, C - immersion heater, D - stirring bar, E - J-tube thermostat, F - gas inlet diffuser, and G - gas outlet through reflux condenser.

before and after each exposure by titration with a 1N NaOH standard. It was found to vary by no more than ± 0.05 normality units from start to finish of any test.

The liquid temperature was controlled to within $\pm 0.35^\circ\text{C}$ by means of an electric thermoregulator coupled to a 100 watt immersion heater.

Immersion tests were conducted in 1N NaCl and 5N HCl. These solutions were chosen because they are nonoxidizing and do not form soluble metal complexes with the exception of CuCl_2^- . Because of the historic significance of dezincification failures in salt water and other chloride environments, it was felt that chlorides should be used despite the existence of this one complex metal ion. The high acid concentration was chosen to minimize acidity changes within the solution. This high acid concentration was also very close to the maximum concentration that can be maintained at 100°C without boiling. (67)

Previous immersion tests in HCl and NaCl have appeared in the literature, (29,40,47,52,61,62,68,69) and comparisons with previous results are contained in the discussion section of this work.

Electrochemical Test Apparatus

The electrochemical hysteresis technique was used for experimental determination of the corrosion behavior of alloys as a function of potential and pH. The equipment, techniques and theories upon which investigations of this type are based have been discussed at some length in other reports.⁽⁷⁰⁻⁷³⁾

The equipment is described schematically in Figure 2 and listed in Appendix 1. The scanning potentiostat applies a continuously varying potential to the sample over a certain range. The differential amplifier isolates the corrosion cell from the recording equipment and eliminates ground loops. The log converter allows the corrosion current to be plotted as a logarithm on the x axis of the x-y recorder, while the sample potential is plotted linearly on the y axis. An automatic step switching apparatus⁽⁷⁴⁾ extends the range of the log converter and allows the continuous recording of corrosion current densities from 5×10^{-8} to 10 amps/cm^2 . The low-pass RC filter, consisting of a 100 microfarad capacitor in parallel with a 25 K-ohm potentiometer adjusted to 10 K-ohms, reduces electrical noise in the system to negligible values.

A schematic diagram of the corrosion cell is seen in Figure 3. The buffered electrolyte is vacuum deaerated prior to transference to the corrosion cell. The solution is continuously purged with hydrogen during the run via the

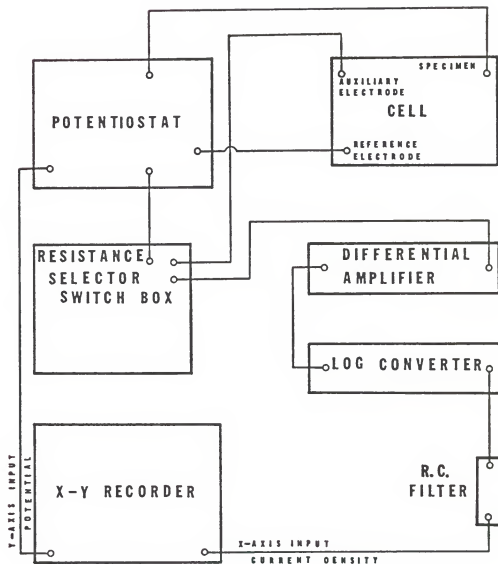


Figure 2. Circuit diagram of equipment used to polarize specimen and automatically record corrosion current density as a function of potential.

CORROSION CELL SCHEMATIC

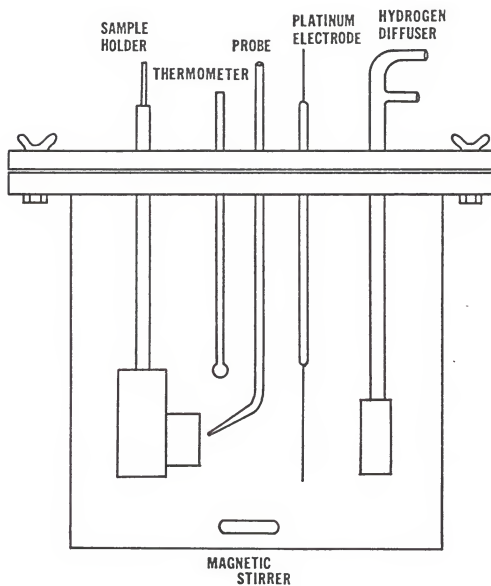


Figure 3. Corrosion cell used in electrochemical investigations.

gas diffuser as suggested by ASTM committee G1.⁽⁷⁵⁾ A bright platinum screen serves as the auxiliary electrode. The current from the potentiostat to the auxiliary electrode is measured as a potential across a precision resistor selected to provide the required logarithmic converter input voltage. A Luggin-Haber probe connected to a standard calomel electrode is used to measure the sample potential. The thermometer is used to indicate the temperature of the electrolyte. The solution is stirred using a magnetic, water-powered stirrer. The cell itself is made of Pyrex glass with a Teflon lid bolted to a polycarbonate Van-Stone backing ring which makes the system airtight.

The sampleholder is shown in Figure 4. The main body of the holder is constructed of Teflon so that it will not react with the test solution. Copper parts encased in the Teflon allow electrical contact with the sample. A polycarbonate nut fastens the sample in place and allows 1 cm² to be exposed to the electrolyte. The Teflon gasket avoids leakage and minimizes crevice effects.

Care must be exercised when choosing buffered electrolytes to insure that solution ions will not form complexes with the metal ions from sample dissolution. The electrolytes used in these studies are listed in Appendix 2. All solutions used in this portion of the investigation had a 0.1 M chloride content. The effects of copper-chloride complexes were discussed in the section on immersion testing.

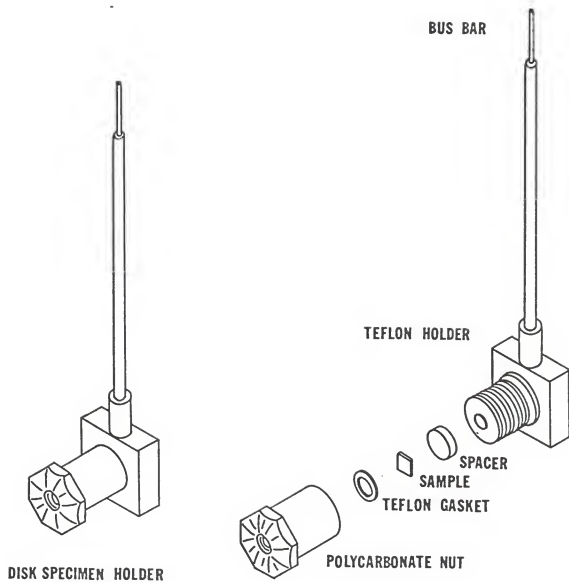


Figure 4. Assembled and exploded views of sample holder.

The effects of scan rate were investigated. Reinoehl and coworkers⁽⁷⁶⁾ show that passivation current density is a function of scan rate, but that critical passivation potentials and rupture potentials are independent of scan rate, at least for iron in 1N H₂SO₄. A more detailed discussion of the importance of scan rates is contained in the discussion section. A scan rate of 33 mv/min was chosen for this investigation after examining scan rates from 5.5 mv/min to 667 mv/min.⁽⁷⁷⁾ The selected rate was slow enough to avoid losing any configuration of the polarization curve, yet fast enough to minimize masking effects due to dezincification of the sample.

After experimental Pourbaix diagrams were established by potentiokinetic polarization techniques, potentiostatic tests were run to verify the potential regions where dezincification occurs. The six-cell potentiostat described by Cusamano⁽⁷²⁾ was used for these potentiostatic tests.

Sample Preparation

The alpha brass samples used in this investigation were donated by the Chase Brass and Copper Company. The brass was obtained in two 25-pound lots of as-extruded cartridge brass wire having diameters of 0.850 in and 0.687 in, respectively. The chemical analyses of these alpha brass samples are shown in Appendix 3.

Beta brass ingots having a nominal composition of 52 w/o Cu and 48 w/o Zn were prepared from 99.99% pure copper and zinc stock purchased from the American Smelting and Refining Company. The ingot melting procedures are described in detail in Appendix 4. The tops and bottoms of each ingot were analyzed according to the procedure described in Appendix 5. Ingots which varied by less than 1.0 w/o Cu from top to bottom were then used in the as-cast condition for these experiments. Each ingot weighed approximately 150 grams and was 15 mm in diameter. The average compositions of the beta brass ingots used are listed in Appendix 6.

Disc-shaped cross-sections were cut from the alpha brass wire and from the as-cast beta brass ingots. Sample surfaces were prepared according to the technique described in Appendix 7.

Five types of samples were used in this study. Samples intended for x-ray analysis were simple discs of brass with a hole drilled through one side so they could be suspended from the sample holder as shown in Figure 1. These samples

were also used for the electron microprobe and optical investigations.

For the atomic-absorption experiments where metal-ion dissolution was to be monitored, cylindrical specimens were mounted in dental mount so as to leave exposed a circular cross-section of known geometric area. The specimens were then polished according to the procedure described in Appendix 7 and suspended in the reaction kettles by means of a hole drilled in the dental mount. This procedure is similar to that described by Fisher and Halperin for their calorimetry studies on the dealloying of copper-gold alloys.⁽⁷⁸⁾

Disc specimens prepared according to the procedure described in Appendix 7 were used for the potentiokinetic experiments using a sample holder shown in Figure 4. For testing details see the section on electrochemical test apparatus.

Early high-temperature tests in this investigation used samples in which all but a 1/2 cm x 1/2 cm square section of the sample was "stopped off" using Miccroshield* stop-off lacquer. Examination of the samples after exposure revealed that leaks through the lacquer were present and this type of sample was abandoned. The significance of these leaks is discussed in the discussion section of this report.

Potentiostatic tests at room temperature were conducted using discs with an insulated copper wire soldered to the

*Trade name, Michigan Chrome and Chemical Company.

back. Miccrostop stop-off lacquer was used to coat the back and sides of these samples leaving a circular exposure surface. Examination of the samples after exposure revealed no apparent leaks in the lacquer.

X-RAY DIFFRACTION

X-ray diffraction and electron diffraction have been used by several researchers in an attempt to ascertain whether dealloying is a process involving the selective removal of one constituent or a dissolution-redeposition process. (38,52,63,64,79-83) If a redeposition process occurs, the diffraction pattern should show diffracted radiation due to remnants of the original alloy and also due to redeposited metal. Diffracted radiation between the two peaks would supposedly indicate an alloy having a composition between that of the original alloy and that of the final, dealloyed, relatively pure metal. This intermediate composition, if detected, would indicate that a selective-removal process is operative.

Most x-ray diffraction and electron diffraction studies of dealloying have involved single-phase, binary alloys of either copper-zinc or copper-gold. The phase diagrams for these two binary systems are shown in Figures 5 and 6.

One of the principal limitations of the copper-zinc system is that alpha brass is stable up to only about 37 w/o zinc at room temperature. This limits the possible changes in lattice parameter, and thus the changes in the resulting x-ray or electron diffraction angles, to a small

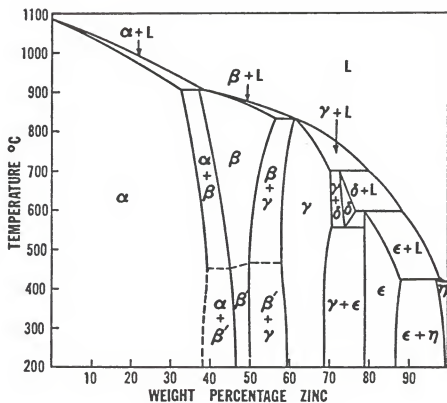


Figure 5. Copper-zinc phase diagram (Metals Handbook, 1948 edition, p. 1206).

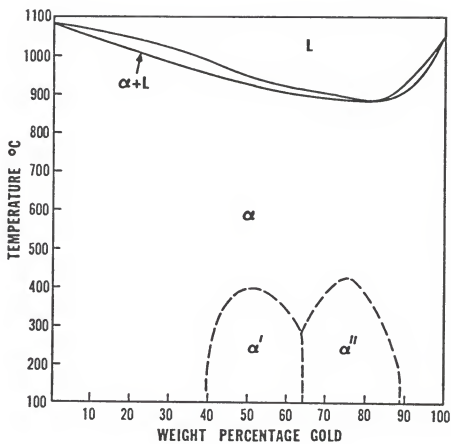


Figure 6. Copper-gold phase diagram (Metals Handbook, 1948 edition, p. 1171).

range.⁽⁸³⁾ The lattice parameter of alpha brass as a function of zinc content is shown in Figure 7.

Pickering points out that by choosing an alloy system, such as copper-gold, with elements having substantial differences in atomic diameter, the lattice parameter, and thus the separation between peaks of the original alloy and those of the corroded residue, will be increased.⁽⁷⁹⁾

An alternative to this would be to start with an alloy which, upon dealloying, would undergo a phase change as well as a change in lattice parameter.

Of the large number of reports concerning diffraction studies of dealloying, only two previous researchers have concluded that their data supported a selective-removal mechanism.^(52,63,64,79)

Pickering subjected copper-gold alloys to electrolytic dissolution and showed the appearance of an intermediate peak which, as additional current was passed, increased in intensity and moved closer to the position to be expected for pure gold. The alloy peak decreased appropriately in intensity.

A later investigation by the same author reported the formation of new, intermediate, phases during the anodic dissolution of gamma brass and of epsilon brass.⁽⁸³⁾ This report substantiated the results of Stillwell and Turnipseed who subjected epsilon brass to various corrosive media, and whose x-ray diffraction results indicated the presence of intermediate phases in some of their experiments.⁽⁵²⁾

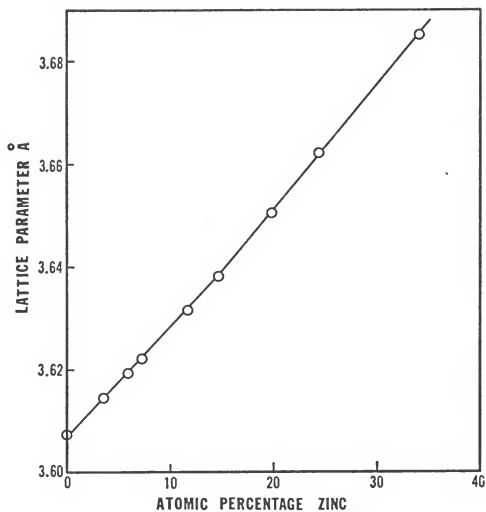


Figure 7. The lattice parameter of alpha brass as a function of the atomic percent zinc. (84)

The lack of similar results in other studies of de-alloying may be due to the use of conventional film methods for recording diffracted intensity. (85)

Present Work

All x-ray diffraction mechanism studies performed during this investigation were performed on powder samples obtained from discs of alpha brass and of beta brass exposed to hydrochloric acid in the immersion apparatus shown in Figure 1 and described in the section on experimental procedure.

There are several problems associated with the use of a diffractometer for investigating dezincification of alpha brasses. If the peaks due to the original alloy occur too close to the copper peaks, then "tails" of diffraction peaks may overlap and be misinterpreted as being due to an alloy of intermediate composition.

This is true of the diffraction patterns obtained using Cu K α radiation. The separation is less than one degree 2θ between the (111) peaks of pure copper and of 70-30 alpha brass. At higher angles the separation between peaks becomes greater, but intermediate intensity, if present, would be spread out also, and thus be harder to detect.

Figure 8 shows the (111) peaks from a sample obtained by mixing filings of alpha brass with annealed filings of copper. A slight increase of intensity due to the overlap of the "tails" of the peaks is apparent.

Figures 9 and 10 show the (111) peaks obtained from samples of alpha brass dezincified for 20 and 30 days, respectively, in 5N HCl at 75°C. The intensity between the

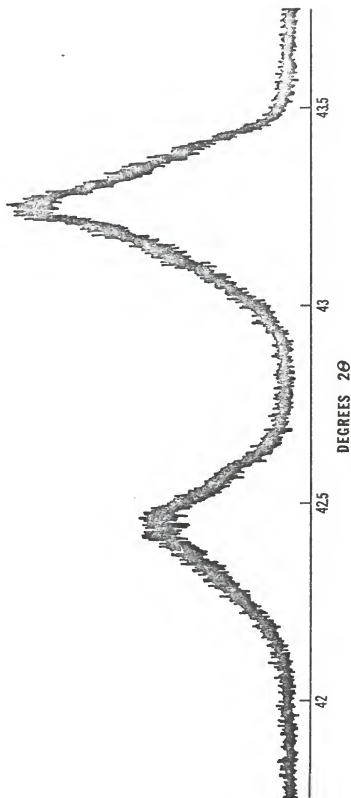


Figure 8. (111) peaks of a mixture of 70-30 brass filings and copper filings. Brass peak is to the left.

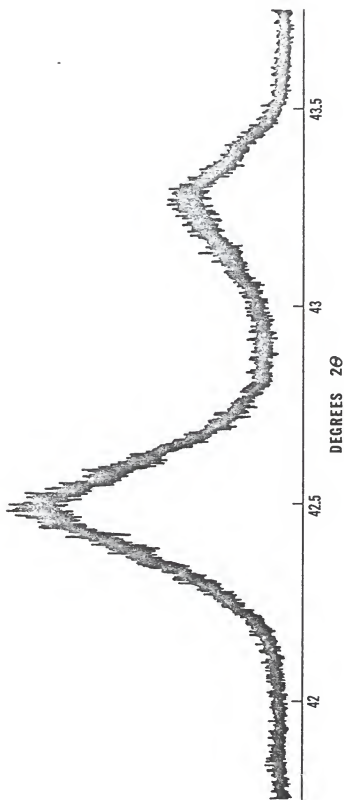


Figure 9. (111) peaks from sample of 70-30 brass dezincified for 20 days in 5N HCl at 75°C.

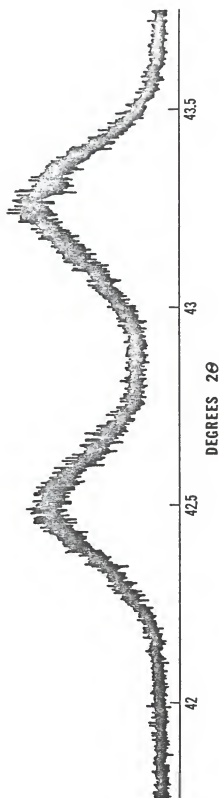


Figure 10. (111) peaks from sample of 70-30 brass dezincified for 30 days in 5N HCl at 75°C.

two peaks on the corroded samples is higher than would be obtained due to overlap of the "tails" of the copper and alpha brass peaks. However, this intensity would probably be undetected on a standard powder pattern obtained by film methods.

If dezincification of beta brass occurs by a volume-diffusion mechanism, the diffraction pattern obtained from a powder of dezincified beta brass could be expected to show scattered intensity characteristic of FCC alpha brass having a lattice parameter different from that of FCC copper. Figure 11 shows a diffraction pattern obtained from a sample of beta brass dezincified for two days in 5N HCl at 75°C. The peak at 43.3 degrees is due to a superposition of beta brass (110) scattering and copper (111) scattering. The broad peak at 42.4 degrees is characteristic of alpha brass having approximately 36 w/o zinc.

The above-mentioned figures thus give x-ray diffraction evidence which supports a selective-removal mechanism for the loss of zinc from both alpha and beta brasses when exposed to 5N HCl at 75°C.

No unidentified peaks were detected in the powder patterns of any of the samples shown above; thus, the possibility of this scattering being due to an extraneous source is eliminated.

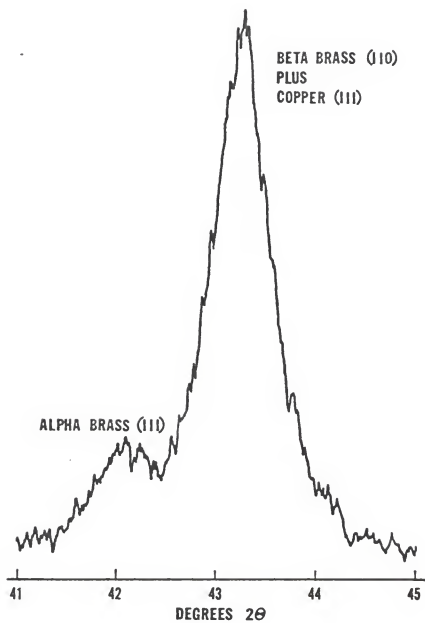


Figure 11. Diffraction pattern from sample of beta brass dezincified for two days in 5N HCl at 75°C.

ELECTRON MICROPROBE

The electron microprobe, with its unique capability for chemical analysis of very small regions, has been used by other researchers in an attempt to show the "diffusion gradients" to be expected from a selective-removal mechanism for dealloying.^(64,79,86)

Birks describes the electron microprobe as having the capability of giving an x-ray spectrochemical analysis of areas between 0.1 and 3 μ in diameter.⁽⁸⁷⁾ The principal factors affecting the size of the region contributing x-rays to the spectrum are the electron beam size and the density of the sample under investigation.

Any quantitative method for x-ray spectrochemical analysis requires comparison with standards having, as nearly as possible, the same physical characteristics as the sample under investigation.⁽⁸⁷⁾ If a selective removal of zinc atoms occurs during dezincification, the atomic sites formerly occupied by these atoms will become vacancies.⁽⁷⁹⁾ As there is no way of reproducing these vacancies, with their subsequent effects on density and surface roughness, in a calibration standard, it is misleading to attempt to assign quantitative chemical analysis values to electron microprobe data from dealloyed specimens.

The use of chart recorders to show diffusion gradients can also be misleading. Both the response time of the chart recorder and the scan rate at which the sample is swept under the electron beam can affect the apparent fall-off distance that is recorded on the chart.

Sugawara and Ebiko⁽⁸⁶⁾ and Pickering^(64,79) have published microprobe data obtained with chart recorders to show relative zinc concentrations as a function of distance. Sugawara and Ebiko concluded that their data gave no indication of a concentration gradient along the interface between corroded and uncorroded brass. Pickering reports a region approximately 9μ thick where the copper concentration fell off in a copper-gold alloy which had been subjected to electrochemical anodic dissolution.

Other researchers have used x-ray images to demonstrate the occurrence of dealloying.^(88,89) None of these authors used microprobe data to support arguments regarding the mechanisms involved.

Present Work

As the above discussion shows, it would be extremely difficult, if not impossible, to obtain meaningful quantitative analyses through electron microprobe analysis of a region having a large, and changing, number of vacancies. This problem has been discussed by Anusavice⁽⁹⁰⁾ who, because of his interest in eliminating vacancy and pore formation in high-temperature diffusion couples, was able to apply pressure and significantly reduce porosity formation.

The technique that was decided upon in this study was to use the University of Florida's Acton Electron Microprobe, operated under conditions which would produce a minimum beam size, to obtain point counts across the region where zinc concentration was found to change. These regions were identified either by using a chart recorder or, as experience was obtained in identifying precise regions of interest, by using the light-optics microscope attachment on the microprobe.

The published data of Pickering^(64,79) and of Forty and Humble⁽⁹¹⁾ indicated that a diffusion zone, if it were to be found, would be rather narrow, of the order of 10μ or even less. Results in these laboratories confirmed these observations and perhaps explain why Sugawara and Ebiko,⁽⁸⁶⁾ who used a chart recorder and a relatively fast scan rate, were unable to find a diffusion zone.

In the present study point counts were taken at intervals as small as one micron across the region of interest. It is recognized that making point counts at narrow intervals might involve some slight overlap of the irradiated volumes between two adjacent points. However, the results obtained by varying operating conditions so that the beam size would be reduced to a bare minimum did not give a change in the results obtained, and it is felt that the counts obtained in this manner are of physical significance.

Results were tabulated as intensity ratios by taking the average of three successive counts on the same point, subtracting the average background intensity on that sample, and dividing by the average point counts on an elemental standard minus the average background intensity on the standard. This can be expressed as:

$$I_A/I_{100A} = \frac{I_A(\text{Sample}) - I_A(\text{Sample BG})}{I_{100A}(\text{Standard}) - I_{100A}(\text{Standard BG})}$$

where A is the element of interest. (87)

Intensity ratios of this type are the raw data for computer programs such as the MAGIC program written by J. W. Colby and in use at the University of Florida for quantitative electron microprobe analysis. (95)

Figures 12, 13 and 14 show plots of intensity ratios versus distance for samples of alpha and beta brass exposed in 5N HCl or in 1N NaCl. The accompanying photomicrographs,

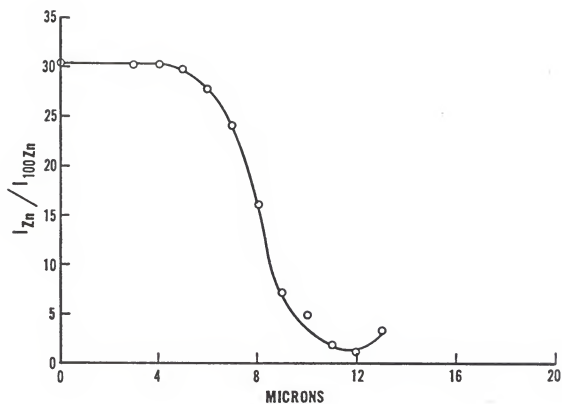


Figure 12. Zinc intensity profile from a sample of alpha brass dezincified for 79 days in 1N NaCl.

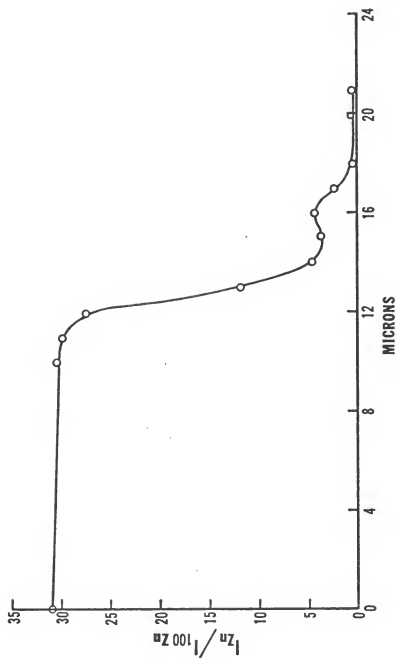


Figure 13. Zinc intensity profile from a sample of alpha brass dezincified for 10 days in 5N HCl at 75°C.

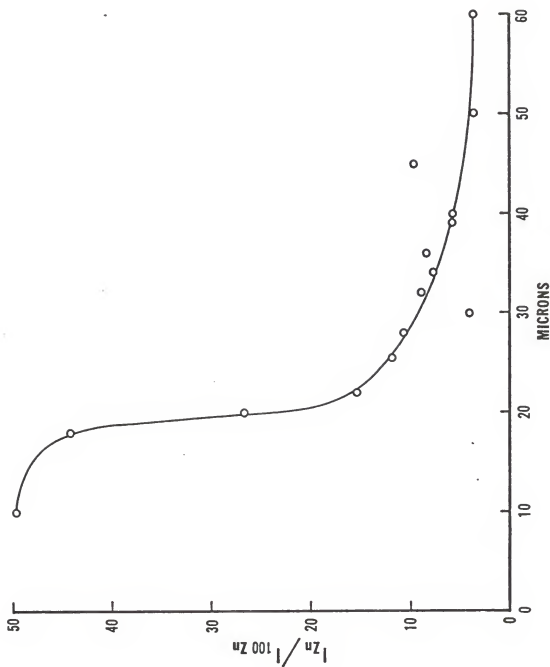


Figure 14. Zinc intensity profile from a sample of beta brass dezincified for two days in 5N HCl at 750°C.

Figures 15, 16 and 17, show the carbon traces left on the sample by the interaction of small amounts of diffusion pump oil with the high-energy electron beam. The diffusion zone occurs in each case at the very edge of the obvious change in color as shown on the photomicrographs.

Figures 12, 13 and 14 are thus, to the author's knowledge, the first experimental plots of alloy composition versus distance to be obtained from samples subjected to dealloying under free corrosion conditions and which indicate the existence of a diffusion zone.

The diffusion distances shown in Figures 12, 13 and 14 are typical of those found on the samples examined. Traces were made across the edges of polished pieces of brass and copper to determine the "distance" which would be recorded due to beam overlap between one-micron settings of the microprobe stage. Results indicated one intermediate point between the intensity ratio of the metal and the background reading on the nonconductive mounting material. A beam at the intermediate-reading setting which was only partially on the sample could explain the intermediate point. The intermediate points of Figures 12, 13 and 14 cover an interval of at least six microns and are thus not due to overlap of the beam at adjacent position settings.



Figure 15. Photomicrograph of sample shown in Figure 12. Probe trace is indicated by the arrow. 500X



Figure 16. Photomicrograph of sample shown in Figure 13. Probe trace is indicated by the arrow. Note surface deposit of copper. 250X

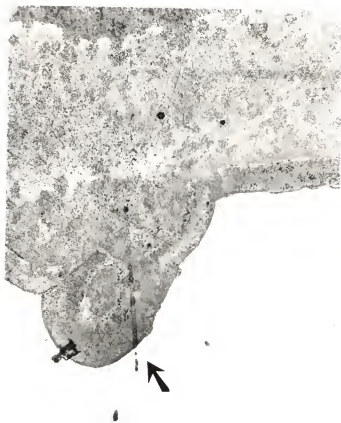


Figure 17. Photomicrograph of sample shown in Figure 14. Probe trace is indicated by the arrow. 250X

OPTICAL METHODS

Early work on the dezincification mechanism relied heavily on optical observations. Most of the research tools used in this study were not developed at that time, but the microscope and metallograph were available and were used. The results obtained from microscopic investigation were, however, subject to "opinion-type" interpretations, and researchers did not have the benefit of present-day knowledge of crystal structure, grain growth, epitaxial electrolytic deposition, the concept of an occluded cell, and other ideas which are part of the present-day researcher's background.

In 1922 Abrams⁽²⁹⁾ suggested that dezincification occurred when a membrane of some type was available to hold dissolved copper in contact with the brass surface or when a large excess of copper was present in the solution. His experiments with copper chloride solutions led to further work by Bengough and May,⁽⁶⁹⁾ and solutions of this type soon became an accepted method of accelerated testing for the susceptibility of alloys to dezincification.⁽⁶⁰⁾

Early researchers noted that dezincification could be classified as occurring either in "layers" or in "plugs" such as the one shown in Figure 18. These plugs were

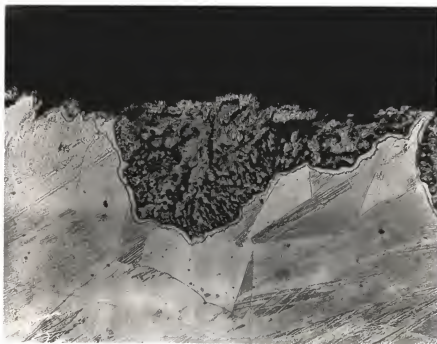


Figure 18. Dezincification plug in 70-30 alpha brass exposed for 79 days in 1N NaCl at room temperature. 200X

attributed to breaks in a protective scale on the metal surface which allowed localized attack in certain specific locations. It seemed obvious that breaks of this type would cause flow restrictions which would lead to a high concentration of copper in a region adjacent to the corroding surface. Bengough and May pointed out that precipitation of copper due to concentration effects seemed likely,⁽⁶⁹⁾ and for a long time this seemed to be the logical mechanism for dezincification. Simmons later pointed out that dezincification plugs occurred under circumstances which, if slightly altered, would result in pits.⁽⁸⁾

Most early investigators were concerned with dezincification of condenser tubes under conditions where scale build-up, and subsequent cracks in the scale, were likely to occur. The ideas put forth by Abrams and by Bengough and May gained wide acceptance. However, this explanation did not seem to cover dealloying in ship propellers and in other high-flow-rate situations.

Interest in the field remained high, and reports of metallographic investigations into the dezincification mechanism continued. Bassett⁽⁴⁵⁾ and Polushkin and Shuldener⁽⁷⁾ decided that dezincification was a selective removal process after examining large numbers of samples which had failed in service. This contrasted with the opinion of Horton⁽³⁹⁾ and served to emphasize that conclusions based on metallographic observation are often dependent on the opinions and prior experience of the observer.

The difficulties of defining and comparing the service conditions reported by various authors are additional drawbacks to arriving at a general mechanism based on optical observations of in-service failures.

In 1965, V. F. Lucey reported on laboratory experiments conducted in closed containers containing saturated copper chloride solutions and containing excess undissolved cuprous chloride.⁽⁴⁰⁾ It is hardly surprising that he observed copper deposition from such a solution.⁽⁹²⁾ However, Lucey neglected to point out that his experiments did not show that a selective removal process could not occur under other circumstances or, indeed, under the conditions described in his papers.

The above discussion is not intended to indicate that optical observations have no value in the determination of a mechanism for dealloying but merely to point out that experiments should be carefully controlled and that limitations of optical methods should be recognized. A concurrent observation is that information which lends support to one theory should not be misinterpreted as proof of the invalidity of a contrasting theory. Some, but by no means all, of the authors discussed above have recognized this, while others, unfortunately, have not.

Present Work

Exposure samples intended for x-ray diffraction analysis were prepared according to the procedures described in the section on sample preparation. NACE Standard TM-01-69⁽⁶⁶⁾ suggests that closed exposure cells, such as were used in this investigation, should contain several samples to be pulled after certain periods of time. Each time a sample is removed from the cell a replacement sample is added. The reason which is given for this is to check for possible changes in the corrosivity of the environment.⁽⁶⁶⁾ As an example, in one series of tests run during this investigation five samples were prepared for each cell. Three were immersed in the original solution. After ten days one sample was removed and replaced with a fresh sample. This was repeated at the end of twenty days, and the test was terminated at the end of thirty days. Thus five samples were obtained from each test and, if no changes in the corrosivity of the environment occurred, the amount of dezincification experienced by the sample exposed for the first ten days of the test would correspond to that of the sample exposed for the last ten. The same should hold for samples exposed for the first twenty days and the last twenty days.

As was mentioned above, these tests were intended primarily as a source of dezincified brass to be used for x-ray powder samples. Because of this each sample was a simple disc with a hole drilled near one edge so it could be

supported in the exposure cell. No effort was made to mask off all but a certain area for exposure and the exposed area was about $19\frac{1}{2}$ cm² in 750 ml of solution ($\sim 2.6 \times 10^{-2}$ cm²/ml) which is quite high. The tests were conducted in 5N HCl at varying temperatures. During these tests a number of the samples appeared to have surface deposits which had a metallic luster and grew larger with the passage of time. These "deposits" were apparent on samples which had been exposed from the beginning of the test as well as on samples which were added when other samples were removed.

Figure 19 shows a photomicrograph of a cross-section of one of these samples. The normal dezincified texture at the bottom of the sample contrasts sharply with the appearance of the shiny surface deposits.

That these formations are, in fact, deposits is shown in Figure 20 where a portion of the original brass surface is visible in the photomicrograph.

Each sample in these tests was weighed before and after the test. The weight-loss data did not follow any recognizable pattern. One sample in these tests actually gained weight.

This particular sample, which was exposed for the last ten days of a twenty-day test, had numerous surface deposits which were copper colored and had a metallic luster.

Figure 21 is a scanning electron micrograph of one of these deposits which fits the "ridge deposition" description

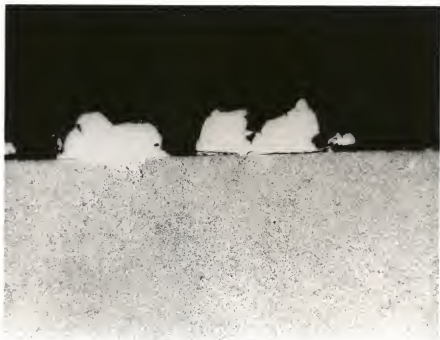


Figure 19. Copper deposits on the surface of dezincified alpha brass sample. Sample was exposed to 5N HCl for 20 days at 100°C. 50X

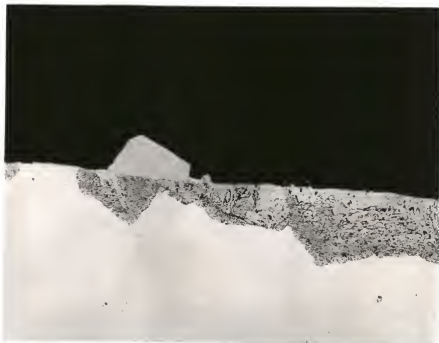


Figure 20. Deposit on surface of dezincified alpha brass sample. Sample was exposed in 5N HCl at 100°C for 10 days. 100X

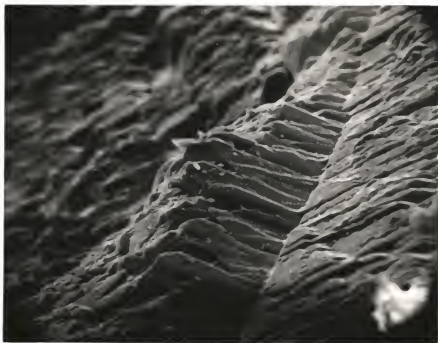


Figure 21. Scanning electron micrograph of copper slab protruding from the surface of a dezincified alpha brass sample. 500X

of copper deposits provided by Bockris and Damjanovic.⁽⁹³⁾ Other deposits had the appearance of "long, curled-up wood shavings." Figure 22 is a nondispersive x-ray pattern of the formation shown in Figure 21, and this pattern clearly shows the deposit to be metallic copper. The sample was exposed to hydrochloric acid in a Pyrex reaction kettle, and the silicon and chlorine peaks are probably due to contamination on the surface of the deposit.

One of the deposits was pulled from the sample surface with a pair of tweezers and made into an x-ray powder sample. The diffraction pattern obtained from this deposit confirmed that the deposits were metallic copper.

Table 1 summarizes the weight change data from the sample discussed above. Figure 23 is a photomicrograph of this sample and shows that the sample did dezincify as well as provide sites for the deposition of copper. No deposits appear in photomicrographs of this sample because they were removed for the x-ray diffraction and weight-change analyses described above.

The above results clearly show that large surface-area-to-cell-volume ratios and the addition of samples to solutions already containing dissolved copper are situations to be avoided. All further tests were conducted on a one-sample-per-cell basis to avoid the effects described above.

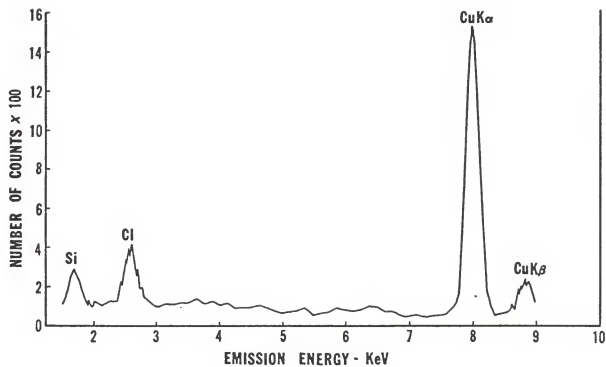


Figure 22. Nondispersive x-ray analyzer pattern of deposit shown in Figure 21.

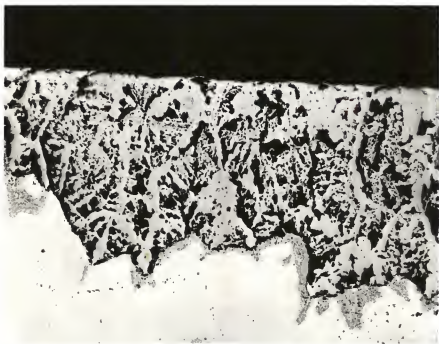


Figure 23. Dezincified cross-section of sample shown in Figure 21. 500X

Table 1
Sample 6-19, Weight Information

Original weight	5.2121 gm
Final weight	5.3901 gm
Weight gained	0.1780 gm
Weight of sample with deposits removed by tweezers and ultra- sonic cleaning	4.5055 gm
Weight of deposits (by difference)	0.8846 gm

SOLUTION ANALYSIS

Chemical changes in the electrolyte surrounding samples undergoing dealloying can provide information regarding the mechanisms involved. Analytical methods which have been used to monitor metal-ion pickup in solution include electrochemical methods [split-ring electrodes^(63,88) and polarography^(44,47,95,96)], colorimetry,^(78,97-100) and radioactive tracer techniques.⁽⁹⁹⁾ Alloy systems investigated include the copper-zinc,^(44,63,88,95,100) copper-gold,^(78,97) and copper-nickel⁽⁴⁷⁾ systems.

Of particular interest is whether or not the more noble species of a binary alloy dissolves during dealloying.^(44,63,78,88,97-99)

Colorimetry and polarography are the only two techniques which have been reported heretofore which can detect the presence of trace elements in solution.^(47,101) Atomic absorption is a technique having detection levels as good as or better than either colorimetry or polarography,⁽¹⁰⁰⁾ and this is the method employed in the present study.

Fisher and Halperin⁽⁷⁸⁾ report that no gold was detected during their colorimetry experiments with copper-gold alloys. This is in agreement with the colorimetric data of Pickering and Byrne on the same system.⁽⁹⁸⁾ By contrast,

copper dissolves from copper-zinc alloys under certain de-alloying conditions. (44,96-97,99)

Marshakov and coworkers⁽⁴⁴⁾ introduced the concept of a "dezincification factor" which can be defined by the equation

$$Z = \frac{(\text{Zn/Cu}) \text{ solution}}{(\text{Zn/Cu}) \text{ alloy}} .$$

The (Zn/Cu) ratio in solution is determined by chemical analysis of the solution, and (Zn/Cu) alloy is the ratio of weight percents of zinc to copper in the alloy. Marshakov and coworkers studied dezincification under a variety of conditions in both NaCl and HCl solutions. They state that alpha brasses in acid media have a dezincification factor slightly in excess of unity. This would mean that the ratio of zinc to copper in solution is slightly greater than it is in alpha brass. No copper was detected in acid solutions which had been in contact with beta and gamma brass ($Z = \infty$). No other reports on solution analysis have appeared for beta brass.

The dissolution of copper from alpha brass has been interpreted as evidence for a redeposition mechanism,^(44,99) or as an indication that the dezincified copper layer was undergoing dissolution.^(47,88,95) Recent radiotracer experiments indicate that exchange of copper between a solution and a copper-containing metal surface can occur.⁽⁹⁹⁾

This would seem to indicate that the presence of copper in solution from a dealloyed metal could also be interpreted as being the result of varying dissolution rates or, in other words, a preferential removal process in which one metal dissolves faster than the other.

Solution analysis has been used to measure the rate of dealloying as a function of time and/or temperature.^(47,78, 95,96) Rubin⁽⁴⁷⁾ reported the "partial apparent heats of activation as a function of composition" for the dissolution of a series of copper-nickel alloys, some of which denickelified, in 1N HCl. The total apparent activation energies, the sums of the two partial values, varied from 5 to 10 Kcal/mole of alloy. The lower figure, corresponding to pure copper, compares quite well with the 5.44 Kcal/mole obtained by Halperin⁽¹⁰²⁾ for the dissolution of copper in ammonia solutions. The values reported are also in the general range described by Vetter for the dissolution of metals in electrolytes.⁽¹⁰³⁾

Fisher and Halperin⁽⁷⁸⁾ reported that copper-gold alloys showed a decrease in dissolution rate with an increase in temperature for all of their alloys. They also observed parabolic corrosion rates. Parabolic corrosion rates are characteristic of systems in which the rate is determined by transfer of reactants through an adherent surface film which thickens as the reaction progresses.⁽¹⁰⁴⁾ Thus they concluded that the rate was limited by a surface film,

probably Cu_2O and/or CuO , which formed under stagnant conditions within the residual gold sponge. Higher temperatures would favor precipitation of copper oxides and the formation of denser film structures, thus accounting for the observed inverse temperature dependence of the reaction kinetics.

The concentration of metal ions in solution has also been used to calculate metal-dissolution currents. (97,98)

The results of these investigations are discussed in the section on electrochemical investigations.

Present Work

Atomic absorption spectrophotometry was used to analyze 5N HCl solutions which had been in contact with freely corroding alpha and beta brasses. Information was obtained on dissolution rates, on the presence or absence of dissolved copper from beta brass, and on the effect of temperature on the reaction kinetics.

While valuable information can be gained from analysis of the electrolyte, this procedure cannot be used as the sole investigative method in the study of dealloying phenomena because of certain severe limitations imposed by the character and structure of the dealloyed metal surface. The morphology of the dezincified copper sponge can have an important effect on dissolution kinetics. The possibility exists that precipitated reaction products can form a surface film which retards dissolution. The surface area of the sponge is substantially greater than that of the alloy at the corrosion interface. This means that sites for the electrodeposition of copper are increased as well as the surface area for dissolution of copper from the sponge. Blocked or narrow passageways can lead to stagnant conditions and the precipitation of salts which would be soluble in the bulk solution. All these effects can alter the metal concentration in the bulk solution, and their possible influence must be considered in the analysis of data on metal dissolution.

The exposure method used for these tests was similar to that reported by Fisher and Halperin.⁽⁷⁸⁾ Reaction kettles were used to expose samples, cut from the same ingot and having the same surface area (2.38 cm^2 for alpha brass, 1.53 cm^2 for beta brass), in 750 ml of argon-sparged 5N HCl at various temperatures. Twenty-five milliliter aliquots of acid were removed from the cells at 12-hour intervals. Each aliquot of sample was replaced with an aliquot of the stock solution used to fill the cell. This caused a dilution of 3.3 % (25 ml out of 750 ml total) each time a sample was removed. Corrections were made for these dilutions in the data which follow.

The aliquots were analyzed using a Heath Model EU-703-D Atomic Absorption Spectrophotometer (see Appendix 1). Both copper and zinc concentrations were determined for each sample.

Data obtained from atomic absorption determinations are tabulated in Tables 2 through 7. Atomic absorption data are reported to only two significant figures consistent with the accuracy of the method.

Figure 24 shows an atomic-absorption calibration curve for copper. This figure shows that copper can be determined to at least the nearest $1/4$ ppm with a reasonable degree of certainty. However, the precision, or the relative accuracy of the measurement when compared to the amount of metal

Table 2
Atomic Absorption Data for Alpha Brass in 5N HCl at 90.35°C

Time (hours)	Amount in solution (ppm)				Weight removed		Total weight removed		Total weight that has been in solution		Amount left in solution		Z
	Cu	Zn	Cu	Zn	Cu	Zn	Cu	Zn	Cu	Zn	Cu	Zn	
12	19	12	12	9	0.48	0.3	0.5	0.3	14	9	14	8.7	1.5
24	25	15	19	11	0.62	0.4	1.1	0.68	19	12	18	11	1.4
36	27	16	21	12	0.69	0.4	1.8	1.1	22	13	20	12	1.4
48	35	18	26	14	0.88	0.4	2.7	1.5	29	15	25	13	1.2
60	38	22	28	16	0.94	0.6	3.6	2.1	31	18	27	16	1.4
72	45	26	34	20	1.1	0.6	4.7	2.7	37	22	33	19	1.3
84	42	28	32	21	1.01	0.7	5.8	3.4	37	24	31	20	1.5
96	45	32	34	24	1.1	0.8	6.9	4.2	39	27	33	23	1.6
108	46	34	35	26	1.2	0.8	8.1	5.1	42	30	34	25	1.6
120	48	36	36	27	1.2	0.9	9.3	6.0	44	30	34	26	1.6

^aAll weights in 10⁻³ gm.

Table 3

Atomic Absorption Data for Alpha Brass in 5N HCl at 98.50°C

Time (hours)	Amount in solution (ppm)				Weight removed				Total weight removed				Total weight that has been in solution				Amount left in solution				Z
	Cu	Zn	Cu	Zn	Cu	Zn	Cu	Zn	Cu	Zn	Cu	Zn	Cu	Zn	Cu	Zn	Cu	Zn	Cu	Zn	
12	20	12.5	15	9.375	.5	.31	.5	.31	.5	.31	.5	.31	.5	.31	.5	.31	.5	.31	.5	.31	1.4
24	40	28	30	21	1	.7	1.5	1.0	3.0	2.1	1.5	1.0	3.0	2.1	1.5	1.0	3.0	2.1	1.5	1.0	1.6
36	80	48	60	36	2	1.2	3.5	2.2	5.8	3.5	3.5	2.2	5.8	3.5	3.5	2.2	5.8	3.5	3.5	2.2	1.4
48	120	67.5	90	50	3	1.7	6.5	3.9	8.7	4.9	6.5	3.9	8.7	4.9	6.5	3.9	8.7	4.9	6.5	3.9	1.3
60	140	77	100	58	3.5	1.9	10	5.8	10.0	5.6	10	5.8	10.0	5.6	10	5.8	10.0	5.6	10	5.8	1.3
72	160	90	120	68	4	2.2	14	8.1	12.0	6.5	14	8.1	12.0	6.5	14	8.1	12.0	6.5	14	8.1	1.3
84	180	100	130	79	4.4	2.6	18	11	13.0	7.6	18	11	13.0	7.6	18	11	13.0	7.6	18	11	1.4
96	200	120	150	88	4.9	3.0	23	14	14.0	8.6	23	14	14.0	8.6	23	14	14.0	8.6	23	14	1.4
108	210	120	160	94	5.2	3.1	29	17	15.0	9.1	29	17	15.0	9.1	29	17	15.0	9.1	29	17	1.4
120	240	140	180	106	6	3.6	34	20	17.4	10.3	34	20	17.4	10.3	34	20	17.4	10.3	34	20	1.4

^aAll weights in 10⁻³ gm.

Table 4

Atomic Absorption Data for Beta Brass in 5N HCl at 59.60°C

Time (hours)	Amount in solution (ppm)				Amount in solution (wt) ^a				Weight removed		Total weight removed		Total weight that has been in solution				Amount left in solution		Z
	Cu	Zn	Cu	Zn	Cu	Zn	Cu	Zn	Cu	Zn	Cu	Zn	Cu	Zn	Cu	Zn			
12	0.75	24	57	1,800	1.9	60	1.9	60	56	1,800	54	1,700	35						
24	1.5	63	110	4,700	3.8	160	5.6	220	110	4,800	110	4,600	46						
36	2	100	150	7,900	5	260	10.6	480	160	10,000	140	7,600	70						
48	2.5	150	188	11,000	6.2	380	17	860	200	12,000	180	11,000	66						
60	3.8	220	280	17,000	9.5	560	26	1,400	300	17,000	280	16,000	64						
72	4	280	300	20,000	10	690	36	2,100	320	22,000	--	--	74						

^aAll weights in 10⁻⁵ gm.

Table 5

Atomic Absorption Data for Beta Brass in 5N HCl at 67.50°C

Time (hours)	Amount in solution (ppm)				Weight removed				Total weight removed				Total weight that has been in solution				Amount left in solution		Z
	Cu	Zn	Cu	Zn	Cu	Zn	Cu	Zn	Cu	Zn	Cu	Zn	Cu	Zn	Cu	Zn	Cu	Zn	
12	1.7	18	130	1,400	4.2	45	4.2	45	4.2	45	130	1,300	120	1,305	11				
24	2.5	50	190	3,800	6.2	120	10	170	10	170	190	3,800	180	3,000	21				
36	3	160	220	12,000	7.5	400	18	570	18	570	240	12,000	220	12,000	56				
48	4	225	300	17,000	10	520	28	1,100	28	1,100	320	17,000	290	16,000	60				
60	4.8	330	360	25,000	12	820	40	1,900	40	1,900	390	26,000	350	23,000	73				
72	5.4	420	400	32,000	13.5	1,000	54	3,000	54	3,000	440	33,000	390	30,000	82				

^aAll weights in 10⁻⁵ gm.

Table 6
Atomic Absorption Data for Beta Brass
in 5N HCl at 89.35°C

Time (hours)	Amount in solution (ppm)				Weight removed	
	Cu	Zn	Cu	Zn	Cu	Zn
12	10	420	780	32,000	26	1,100
24	32	1,200	2,400	94,000	80	3,100
36	60	2,000	4,500	150,000	150	5,000
48	100	2,800	7,500	210,000	250	7,100

^aAll weights in 10^{-5} gm.

Table 6 (Extended)

Total weight removed		Total weight that has been in solution		Amount left in solution		Z
Cu	Zn	Cu	Zn	Cu	Zn	
26	1,100	780	32,000	750	31,000	44.6
110	4,200	2,400	95,000	2,300	91,000	42.6
260	9,200	4,600	150,000	4,440	140,000	36.5
510	16,000	7,800	220,000			31.3

Table 7

Atomic Absorption Data for Beta Brass
in 5N HCl at 99.85°C

Time (hours)	Amount in solution (ppm)				Weight removed	
	Cu	Zn	Cu	Zn	Cu	Zn
12	34	1,200	2,500	94,000	84	3,100
24	150	3,100	11,000	230,000	380	7,800
36	380	4,600	28,000	350,000	940	11,500
48	820	5,500	62,000	410,000	2,100	14,000

^aAll weights in 10^{-5} gm.

Table 7 (Extended)

Total weight removed		Total weight that has been in solution		Amount left in solution		Z
Cu	Zn	Cu	Zn	Cu	Zn	
84	3,100	2,500	94,000	2,400	91,000	40.70
460	11,000	11,000	240,000	11,000	230,000	22.85
1,400	22,000	29,000	360,000	27,000	340,000	13.64
3,500	36,000	63,000	430,000	--	--	7.50

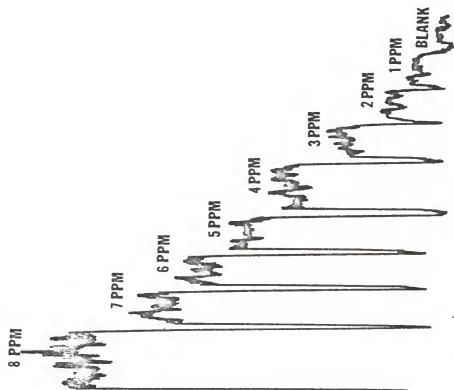


Figure 24. Atomic-absorption calibration curve for copper.

available for measurement, is lower for more dilute samples. As an example, a $1/4$ ppm deviation in a sample having 2 ppm copper yields a $12-1/2$ percent error, whereas in a sample having 8 ppm copper the same $1/4$ ppm deviation would produce an error of only $3-1/8$ percent. This type of precision deviation is common to all atomic absorption methods. The confidence limits shown on the figures which follow were calculated by assuming a possible $\pm 1/4$ ppm deviation for the original instrument reading obtained on the sample in question.

The Heath spectrophotometer is a single-beam instrument. This means that no provision is made for automatically adjusting for instrumental drift due to power deviations or lamp fluctuations.⁽¹⁰⁵⁾ It was found in practice that the instrument would drift significantly in a short period of time, thus negating the value of a calibration curve. For this reason, a procedure was developed whereby each sample was introduced into the absorption flame once to determine the general range of the concentration of the element being analyzed. Then standards were introduced into the flame to confirm the concentration range of the unknown. The values tabulated in Tables 2 through 7 were then determined by introducing one standard, then the unknown, and then another standard, so that each unknown reading was bracketed by two standard readings.

The limits of detection for the unit under the operating conditions used in this investigation were approximately 0.15 ppm for zinc and approximately 0.25 ppm for copper. Theoretical limits of detection for these elements by atomic absorption are somewhat lower than this, but the solutions analyzed had copper and zinc contents well above these limits, and most of them required dilution to be brought within the operating range of the instrument.

Figure 25 shows the dilution-corrected values for copper and zinc dissolved from alpha brass at various times (see also Column 4 of Table 3). The zinc values obey linear kinetics, but the copper values fluctuate.

Copper and zinc dissolution from alpha brass at 98.50°C is shown in Figure 26. Once again, linear kinetics are observed for zinc, and the copper values fluctuate somewhat before they too become linear.

The dezincification factor, Z , that was introduced by Marshakov and coworkers⁽⁴⁴⁾ is plotted for this cell in Figure 27. When the confidence limits are taken into consideration, Z for alpha brass is seen to be between 1 and 1.5 for this investigation. This is in general agreement with Marshakov and coworkers. The usefulness of determining Z is limited since the absolute magnitudes of the values of Z are strongly influenced by the precision of chemical analysis methods in processes (such as dealloying) where the quantities being analyzed are small.

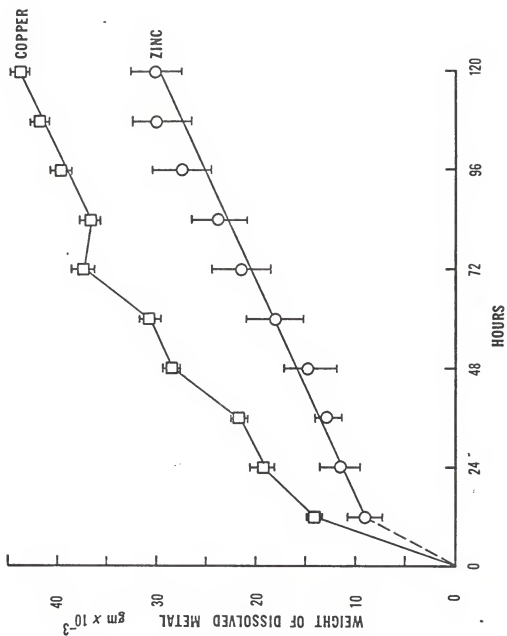


Figure 25. Copper and zinc dissolution from alpha brass in 5N HCl at 90.35°C. Scatter bands show the precision of the original measurements.

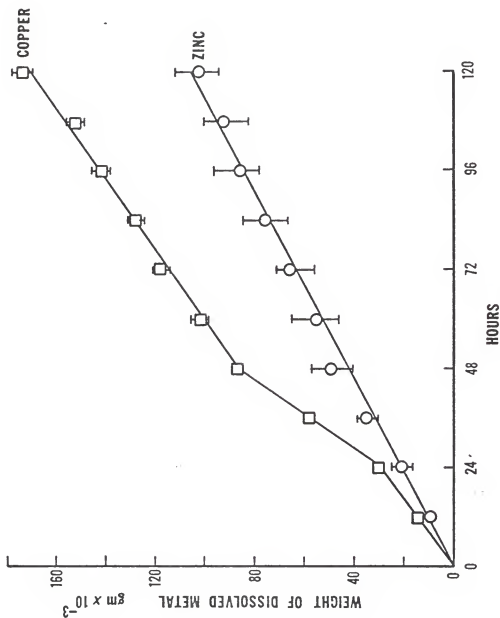


Figure 26. Copper and zinc dissolution from alpha brass in 5N HCl at 98.50°C. Scatter bands show the precision of the original measurements.

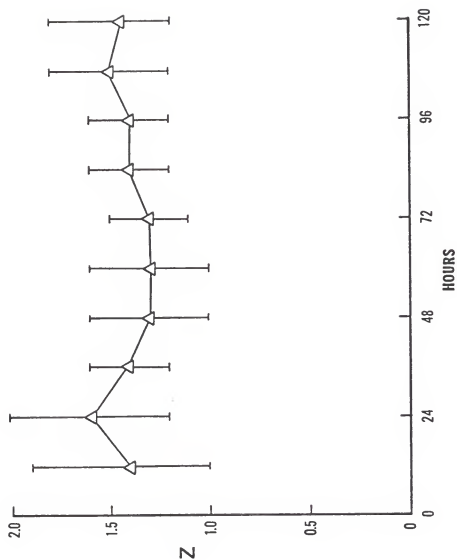


Figure 27. Dezincification factors, Z , for alpha brass in 5N HCl at 98.50°C. Scatter bands show the limits of precision for the original measurements.

Figures 28 and 29 show the corrected amounts of copper and zinc which have dissolved from beta brass at 67.50°C as a function of time. They are not plotted on the same scale, as was done in Figures 25 and 26 for alpha brass, because the dissolution rate for zinc (Figure 29) is much greater than the dissolution rate for copper (Figure 28). The reaction kinetics for both copper and zinc appear to be linear after the first 24 hours.

Slight fluctuations in the copper or zinc dissolution kinetics make disproportionately large changes in the magnitudes of the dezincification factor Z . This is seen in the positions of the calculated points in Figure 30. The values shown in Figure 30 for beta brass are up to fifty times the values plotted in Figure 27 for alpha brass. It is emphasized here that the values for beta brass are finite in contrast to the results of Marshakov and coworkers who reported dezincification factors which were infinite for beta brass because no dissolved copper was detected by them. This again illustrates that Z has no fundamental significance with regard to the mechanism of dealloying.

The effect of temperature on the dissolution kinetics of zinc from beta brass is shown in Figure 31 where the amount of zinc dissolved for beta brass is plotted versus time for four different temperatures. There is an obvious increase of zinc dissolution rate with temperature.

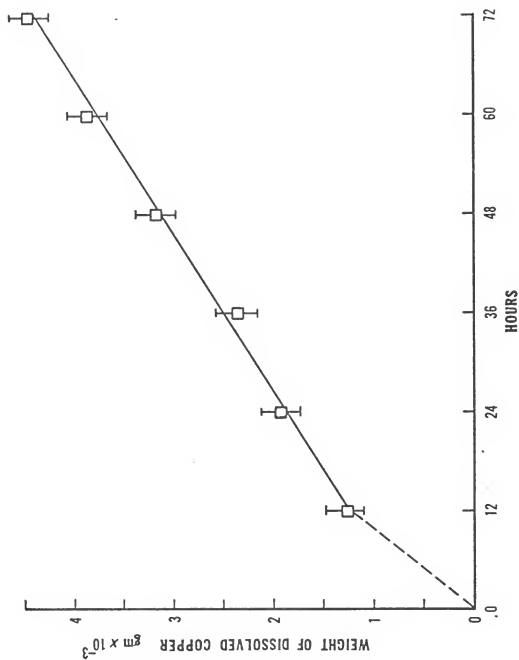


Figure 28. Copper dissolution from beta brass in 5N HCl at 67.50°C.

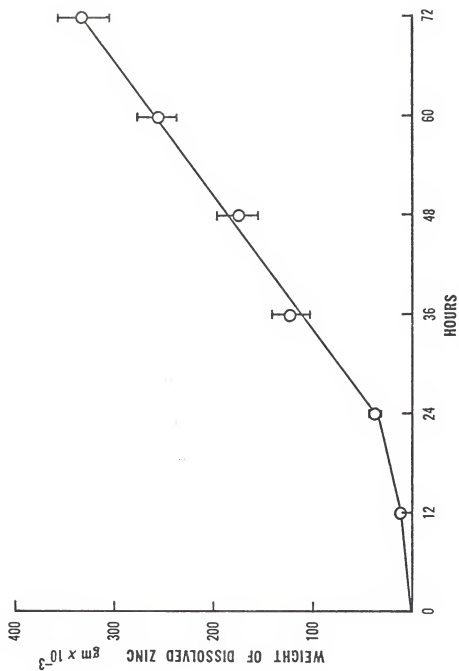


Figure 29. Zinc dissolution from beta brass in 5N HCl at 67.50°C.

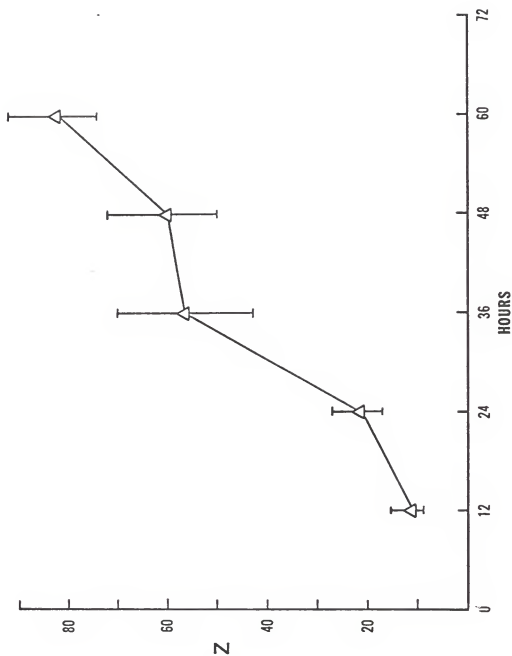


Figure 30. Dezincification factors, Z , for beta brass in 5N HCl at 67.50°C. Scatter bands show the limits of precision for the original measurements.

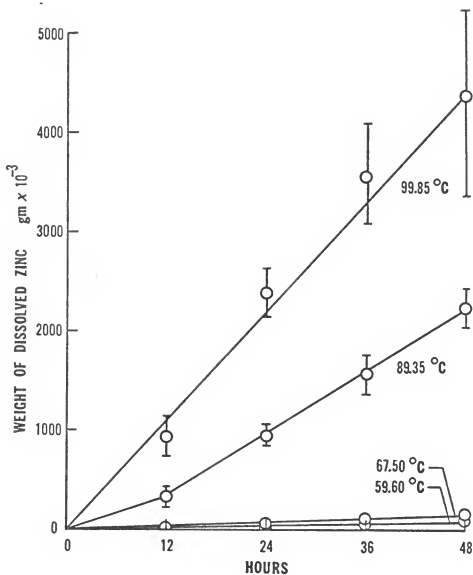


Figure 31. Zinc dissolution from beta brass in 5N HCl at various temperatures. Scatter bands show the limits of precision for the original measurements.

Many chemical reactions, including metal dissolution, are found to obey an empirical equation first proposed by Arrhenius

$$K = K_0 e^{-Q/RT},$$

where the pre-exponential factor, K_0 , is usually found to be temperature-independent, at least within the experimental accuracy of the observations,^(104,106) and Q is the so-called "activation energy." K and K_0 in the above equation are rate-related measurements such as weight loss, weight gain, depth of penetration, and metal dissolution for corrosion experiments. The amount of zinc dissolved in 48 hours was used in the discussion which follows. This is a reasonable choice since Figure 31 shows the kinetics to be linear. R in the Arrhenius equation is the gas constant, 1.986 calories gm-mole⁻¹ degree K⁻¹,⁽¹⁰⁴⁾ and T is the absolute temperature in degrees Kelvin.

If reaction kinetics can be represented by the above Arrhenius formula, then a plot of $\log K$ as a function of $1/T$ will give a straight-line having a slope of $-Q/2.303R$.^(104, 106)

Figure 32 is an Arrhenius plot of the amount of zinc dissolved from beta brass in 48 hours. The activation energy for zinc dissolution over the temperature interval 59.60-99.85°C is found from the slope of this graph to be 18 Kcal gm-mole⁻¹. This value is somewhat higher than those for

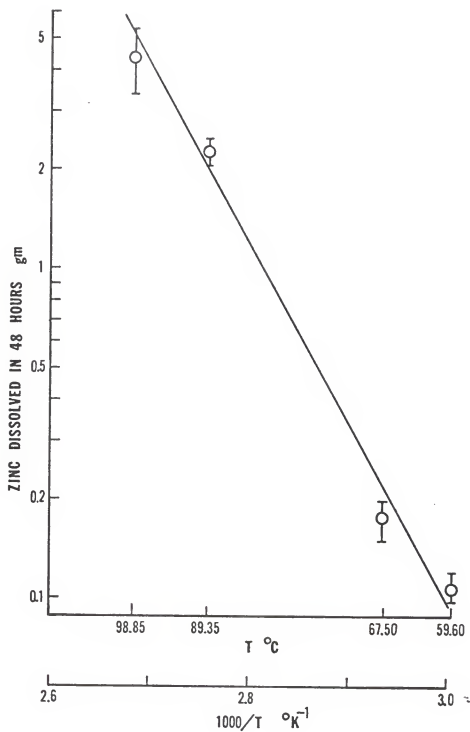


Figure 32. Arrhenius plot of zinc dissolution rate versus $1000/T$. Scatter bands show the limits of precision for the original measurements.

electrochemical metal dissolution (± 10 Kcal gm-mole⁻¹), (103) the dissolution of copper-nickel alloys as reported by Rubin (5-10 Kcal gm-mole⁻¹), or the dissolution of copper reported by Halperin. (102)

Kofstad points out the difficulty of ascribing physical interpretations to experimentally determined activation energies. (104)

Several conclusions can be drawn from the atomic-absorption data. There can be no doubt that at least some copper enters solution from both alpha and beta brass when freely exposed under conditions used in these tests. This contradicts the results of Marshakov and coworkers⁽⁴⁴⁾ who reported that no dissolved copper was detected in solution for their experiments with beta brass in 0.5M NaCl and in 0.5M HCl.

There is evidence for a linear dissolution rate for zinc from both alpha and beta brasses (see Figures 25, 26, 29 and 31). This would support the metallographic observations of Langenegger and Robinson. (62)

The irregular dissolution kinetics for copper seen in Figures 25, 26, 27 and 30 are believed to be due at least in part to the effects of the morphology of the "spongy" dezincified surface on the corrosion processes.

A comparison of the data obtained from alpha and beta brasses confirms that beta brass corrodes much more rapidly than does alpha brass in hydrochloric acid.

The dezincification factor introduced by Marshakov and coworkers provides an indication of whether or not dezincification has occurred.

However, the factor Z has no fundamental significance and the absolute magnitude of the dezincification factor may vary considerably for a given exposure cell and cannot be compared with the values from other cells. The sensitivity of the dezincification factor to the irregularities of the dissolution kinetics of copper during dezincification is well illustrated.

ELECTROCHEMICAL INVESTIGATIONS

Early electrochemical tests measured the potential of brasses in solutions known to produce dezincification.⁽⁶⁹⁾ At that time it was not generally recognized that duplex alloys, such as alpha-plus-beta brasses, would exhibit microstructure-dependent electrochemical behavior.

In 1967, Joseph and Arce⁽¹⁰⁷⁾ showed that the corrosion behavior of a 63 w/o Cu - 37 w/o Zn brass was strongly dependent on structure. This particular alloy can have either a single-phase alpha or a duplex alpha-plus-beta structure, depending on heat treatment, as revealed in the copper-zinc phase diagram, Figure 5. Several recent electrochemical studies of dealloying have examined the behavior of single-phase copper alloys and of more complex copper alloys and have taken microstructure into account.^(44,97,103-110)

Some researchers have used driven anodes as a rapid means of producing specimens to be examined by non-electrochemical means.⁽⁶²⁻⁶⁵⁾ Others have used electrochemical observations to arrive at conclusions as to the mechanism of dezincification.^(43,88,95,96,112) Still others have tried to define current,^(4,98,112) potential,^(44,86,97,98,110,113) or potential-pH^(58,86,114,115) conditions where dealloying

might be expected to occur, or to determine potentials where cathodic protection may be possible. (3,116-119)

Electrochemical tests have a number of drawbacks and may be subject to misinterpretation. For example, constant-potential tests conducted for short periods, e.g., two hours, at room temperature which fail to produce observable dezincification⁽¹⁰⁾ may produce measurable dezincification after longer periods of time. (3,44,86)

Electrochemical tests on alloys subject to dealloying have an added difficulty in that the surface of the sample will quickly change to that of a dealloyed metallic "sponge" if the electrode is subjected to dealloying conditions. (44,86, 98,113) Sugawara and Ebiko⁽⁸⁶⁾ point out that thick anodic films, such as those caused by dezincification, may produce additional resistance, and thus a potential drop, between the surface and the uncorroded portion of the sample. This means that the true potential of the uncorroded sample cannot be determined. However, this potential change, which is expressed by Ohm's Law, $E = IR$, is very small, because the currents being measured in a typical electrochemical cell are of the order of 10^{-8} to 10^{-2} amperes. (71,98)

Wilde and Teterin⁽¹¹³⁾ reported that their anodic polarization curves for alpha brasses and duplex alpha-plus-beta brasses were almost identical with the curve for pure copper. The only measurable differences were in current density. They attributed the similarities to a copper layer

which formed on the sample surfaces. Similar results were reported by Sugawara and Ebiko⁽⁸⁶⁾ for alloys in the same composition range. Alloys having 47 w/o zinc (beta brass) or more were reported as having anodic polarization curves which became more like that of zinc as the zinc composition increased.

Marshakov and coworkers⁽⁴⁴⁾ stated that "The anodic behavior of alloys is determined by the rate of dissolution of the noble component as the slowest stage." They investigated single-phase alpha and beta brasses as well as duplex alpha-plus-beta brasses.

Pickering and Byrne⁽⁹⁸⁾ investigated the effects of a dealloyed sponge on the surface of a sample by holding copper-gold alloys at dealloying potentials for varying periods of time and then "jumping" the potential to a more noble level. They showed that below a certain "critical potential" the copper-dissolution current from copper-gold alloys was dependent on the rate of copper solid-state diffusion from the alloy. Above the critical potential the copper-dissolution current became strongly potential-dependent. This critical potential was shown to be composition-dependent for the copper-gold alloy system, which is a homogeneous alloy system over the composition range investigated, as well as for copper-zinc alloys,⁽⁹⁷⁾ where phase changes could be interpreted as causing shifts in the critical potential.

Some of the potentials that Pickering and Byrne investigated were below the hydrogen evolution potentials for the electrolytes they used. Because there was no accurate way to subtract the hydrogen-evolution current from the measured electrode current, they used chemical analyses of the metals in solution to determine dissolution currents. This also allowed them to plot the dissolution currents for each dissolving species separately at potentials where the more noble metal in the alloy was also dissolving.

Potential-versus-pH plots (Pourbaix diagrams) of regions of chemical stability of elements, their ions, and their salts in aqueous environments, present one possible way of providing a basis for predicting the tendency for dealloying. Latanision and Staehle,⁽¹¹⁴⁾ Verink and Parrish,⁽¹¹⁵⁾ and Verink and Heidersbach⁽⁵⁸⁾ have suggested that the superposition of Pourbaix diagrams⁽¹²⁰⁾ for the constituent elements of the alloy may reveal a region of potential and pH where one element would tend to corrode while the other(s) would be immune. Latanision and Staehle later concluded that their hypothetical denickelification of Fe-Ni-Cr alloys was not substantiated by their experimental observations.⁽¹²¹⁾ However, the copper-nickel system suggested by Verink and Parrish and the copper-zinc system discussed by Verink and Heidersbach both are widely reported to dealloy in service.^(2,13-15,89,122,123)

Another advantage of the Pourbaix diagram, or potential pH, approach to dealloying is that information obtained by various authors in different solutions can be plotted in a manner which provides meaningful correlations.

Present Work

The experimental potential-pH (Pourbaix) diagram for 70 w/o Cu - 30 w/o Zn alpha brass in 0.1M chloride solutions is shown in Figure 33 and was determined by W. C. Fort, III,⁽⁷⁷⁾ according to the method of Pourbaix.⁽¹²⁰⁾ Figure 34 is a simplified version of the equilibrium diagram calculated by van Muylder, Zoubov and Pourbaix⁽¹²³⁾ assuming a chloride ion concentration of 0.1M and all other ionic species to be present in 10^{-6} M concentrations. Figure 35 is a similar simplified diagram for the zinc-H₂O systems.⁽¹²⁰⁾ Figures in the diagrams correspond to calculations which are listed in Appendix 8. Superposition of diagrams, Figures 33, 34 and 35, gives Figure 36. It is evident that the experimentally constructed diagram shows a number of features in common with the equilibrium (potential versus pH) diagram for copper. Verink and Heidersbach have discussed these similarities at some length.⁽⁵⁸⁾

For pure copper in deaerated solutions, the zero current potential on the upward potential sweep of the electrochemical hysteresis circuit indicates the position of the so-called "immunity" line at a given pH. The potential at which this zero current is observed often is fairly close to the calculated position of the metal/metal ion coexistence potential for a metal ion concentration of 10^{-6} molar. Thus the arbitrary choice of 10^{-6} molar as a definition of

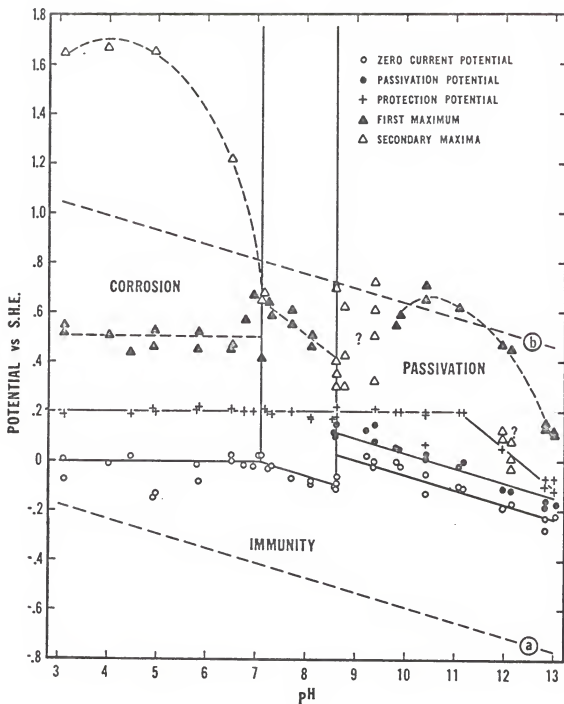


Figure 33. Experimental potential versus pH diagram for 70 Cu - 30 Zn in 0.1M Cl^- at 25°C. (77)

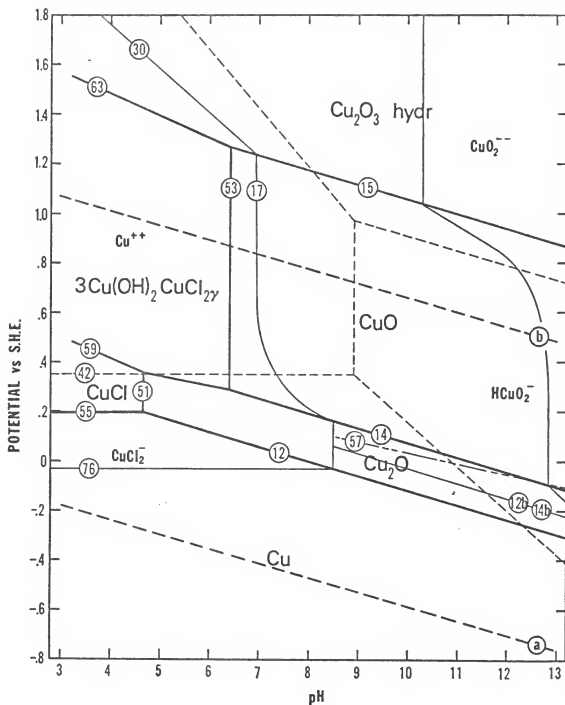


Figure 34. Simplified Cu-Cl-H₂O diagram at 25°C for solution containing 0.1M chloride ions; concentrations of ionic species = 10⁻⁶M. [Redrawn from Ref. 123.]

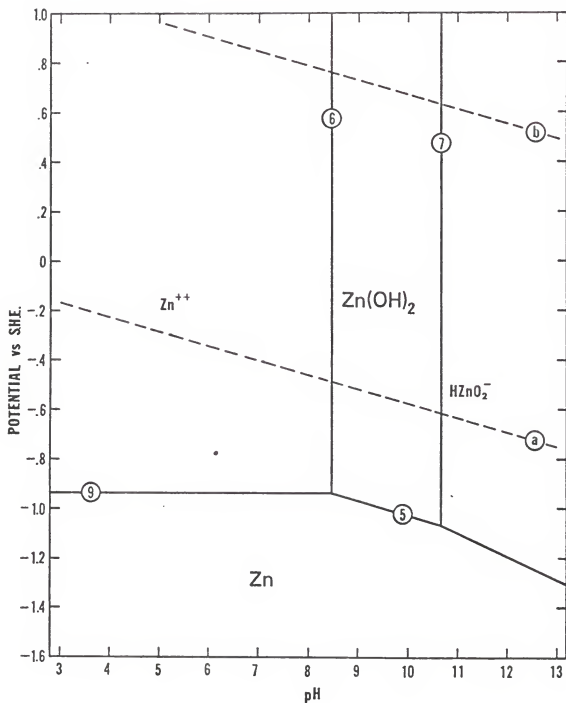


Figure 35. Simplified Zn-H₂O diagram for concentrations of ionic species = 10⁻⁶M.

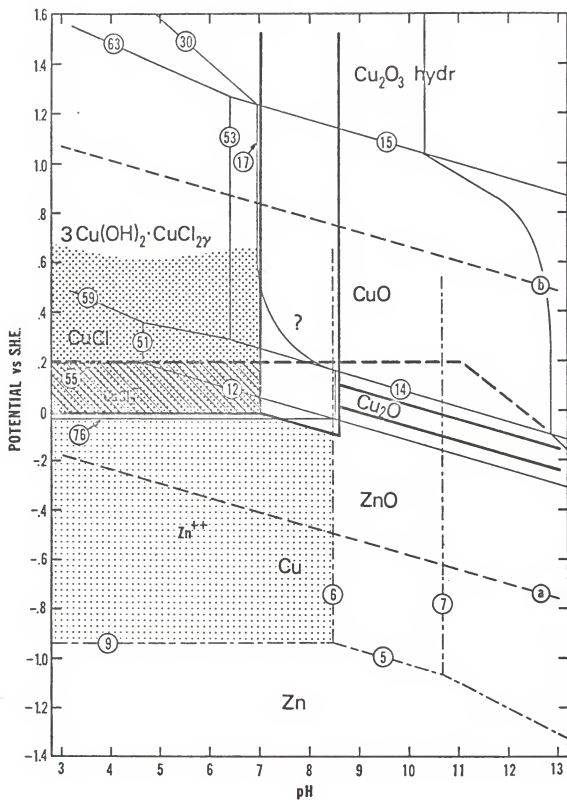


Figure 36. 70 Cu - 30 Zn alloy in 0.1M chloride solution. Superposition of the experimental potential diagram, Figure 33, onto Figures 34 and 35.

"noncorrosion" seems appropriate. Alloys which are rich in one component (e.g., 70-30 Cu-Zn or 90-10 Cu-Ni) tend to have many features in common with the diagram for the major component (in this case, copper). The "immunity" line, however, appears to have a somewhat different significance for alloys than for pure metals. While the kinetics of alloy dissolution for alpha brass are slow below the alloy "immunity" line, this does not rule out the possibility of dealloying. Referring to Figure 37, the "immunity" line for 70-30 Cu-Zn in 0.1M chloride was about $0.000V_{SHE}$. Between this potential and approximately $-0.940V_{SHE}$ (line #9) there is a theoretical tendency for the selective removal of zinc from the alloy.

At potentials more positive than about $0.000V_{SHE}$, both constituents of the 70-30 Cu-Zn alloy go into solution. Pickering and Byrne⁽⁹⁷⁾ report that "two modes of dissolution may occur depending on the potential: preferential and simultaneous. Preferential dissolution changes gradually with potential from virtually no dissolution of the more noble metal to simultaneous dissolution of both components." Pickering and Byrne observed this change in behavior between $+0.050V_{SHE}$ and $+0.200V_{SHE}$ in Na_2SO_4 solutions at pH 5. There were no chloride ions in their solutions, but the potential-pH conditions they described fit into the cross-hatched area on Figure 36.

If the above-stated hypotheses are correct, then 70-30 brasses should be expected to undergo dezincification in acid solutions at potentials from $\approx -0.940V_{SHE}$ to $0.200V_{SHE}$ (the region with small dots on Figure 36). At potentials between $0.000V_{SHE}$ and $+0.200V_{SHE}$ (the cross-hatched region of Figure 36), copper and zinc should dissolve, but not necessarily in the same ratio as in the alloy.

In order to test these hypotheses, a series of potentiostatic tests of alpha brass were conducted in buffered 0.1M chloride solutions at pH 4 (see Appendix 2 for the exact composition of the solution used).

The equipment for these tests and the sample preparation procedures were discussed in the section on experimental procedure.

The results of these tests are tabulated in Table 8. The samples exposed at $+0.150V_{SHE}$ and $+0.050V_{SHE}$, in the domain described by the cross-hatched region of Figure 36, appeared dezincified in solutions that were not stirred. Stirred solutions produced samples which appeared to have undergone general dissolution. Stirring apparently removed stagnant conditions which would allow redeposition of copper on the specimen surface.

Those samples which were exposed at potentials from $-0.050V_{SHE}$ to $-0.850V_{SHE}$ were observed to dezincify in stirred solutions. This corresponds to the potential region where Pickering and Byrne⁽⁹⁷⁾ reported dezincification of

Table 8

Alpha Brass Potentiostatic Test Data

Potential E _{SHE}	Dezincified Surface Appearance?	Was Solution Stirred?	Duration of Exposure	Zinc in Solution?	Copper in Solution?	Copper on Platinum Electrode?	Remarks
+0.150	No	Yes	22 hours	Yes	Yes	Yes	
+0.150	Yes	No	22 hours	Yes	Yes	Yes	
+0.050	No	Yes	5 days	Yes	No	Yes	
+0.050	Yes	No	5 days	Yes	No	Yes	
-0.050	Yes	Yes	10 days	Yes	No	No	
-0.050	Yes	No	10 days	Yes	No	No	
-0.750	?	Yes	8 days	Yes	No	No	Surface has black tarnish at end of test
-0.850	?	Yes	12 days	Yes	No	No	Surface has black tarnish at end of test
-1.050	?	Yes	13 days	Yes	No	No	Surface has gray tarnish which turns black when dry

alpha brass by the selective removal of zinc. Zinc ions were present but no copper was detected at these potentials, either on the platinum auxiliary electrode or by atomic-absorption analysis of the bulk solutions. Clearly selective dissolution of zinc is the predominant process in this potential range.

Certain of the samples exhibited a dark tarnish ($-0.750V_{SHE}$ and $-0.850V_{SHE}$). These are presumed to have undergone dezincification, although the tarnish film was too thin for unequivocal identification by x-ray analysis.

Superposition of Pourbaix diagrams of copper and zinc also was used to assess the dealloying behavior of beta brass. Although a complete experimental Pourbaix diagram was not available for beta brass, enough data were at hand to facilitate selection of appropriate potentials for potentiostatic studies in 0.1M chloride solutions at pH 4.

The results of these studies are shown in Table 9. All samples exposed to potentials from $+0.050V_{SHE}$ to $-0.850V_{SHE}$ were found to dezincify. The effects of stirring were not as obvious as for alpha brass, but between $+0.050$ and $-0.150V_{SHE}$ in stirred solutions copper was deposited on the platinum auxiliary electrode. The lowest potential at which copper was detected on the platinum auxiliary electrode in stirred solutions was $-0.150V_{SHE}$. Evidently the high zinc content in beta brass causes this potential to be more active than was found to be the case for alpha

Table 9
Beta Brass Potentiostatic Test Data

Potential E _{SHE}	Dezincified Surface Appearance?	Was Solution Stirred?	Duration of Exposure	Zinc in Solution?	Copper in Solution?	Copper on Platinum Electrode?	Remarks
+0.050	Yes	Yes	1 day	Yes	ND	Yes	
+0.050	Yes	No	1 day	Yes	ND	No	
-0.050	Yes	Yes	2 days	Yes	ND	No ^a	
-0.050	Yes	No	2 days	Yes	ND	No	
-0.100	Yes	Yes	3 days	Yes	ND	Yes	
-0.150	Yes	Yes	3 days	Yes	ND	Yes	
-0.250	Yes	Yes	6 days	Yes	ND	No	
-0.250	Yes	No	6 days	Yes	ND	No	
-0.850	?	Yes	13 days	Yes	ND	No	Red tarnish after one day is black by end of test
-1.050	?	Yes	7 days	Yes	ND	No	Silver-gray tarnish visi- ble after one day. Remains silver after drying.

^aComparison with the test at -0.100V_{SHE} suggests that copper might have been found on the platinum electrodes after longer periods of time.

brass. In unstirred cells the copper appeared to have remained at or near the sample surface, since no copper was detected in the bulk solutions, after any of the potentiostatic beta brass tests.

Figure 37 shows the surface of a sample of beta brass which was held in a sample holder such as is shown in Figure 4. The sample was exposed for a short-term test of 2-3/4 hours at $+0.050V_{SHE}$. The reddish copper crescent in the upper left of the photograph illustrates the effects of stirring on dezincification. That portion of the sample surface which was sheltered from stirring by the configuration of the sample holder (i.e., a relatively stagnant area) has a dezincified appearance due to the deposition of copper. Where stirring was effective (the balance of the surface) dezincification did not occur.

The above photograph, coupled with the observations on alpha brass discussed above, can be taken as further evidence that dezincification can occur by an electrodeposition mechanism in certain potential ranges.

Figure 38 shows the configuration of a typical potentiokinetic scan for alpha brass. Plots of the zero current potential on the return (downward) scan, E_p , are shown by the line numbered 55 in Figure 34 and in Appendix 8.

At this potential on downward potentiokinetic scans the samples were observed to change to a reddish color

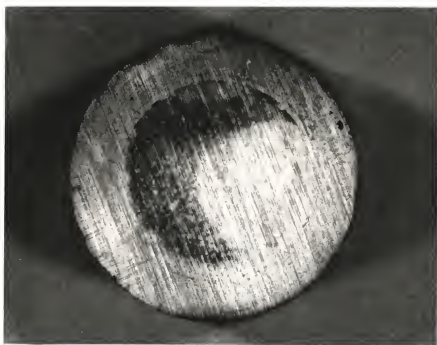


Figure 37. Beta brass held at $+0.050V_{SHE}$ for 2-3/4 hours. Crescent-shaped reddish region shows effect of stirring action on dezincification.

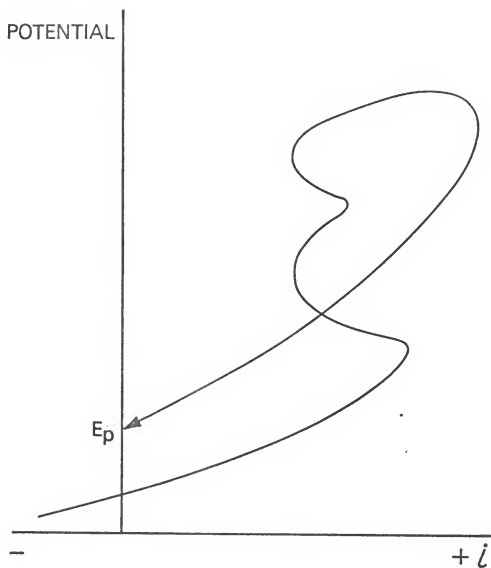


Figure 38. Typical potentiokinetic scan in acid solutions. E_p is found to occur near $+0.200V_{SHE}$ and between the zero-current potential and the first maximum.

typical of copper deposits. This potential is approximately $+0.200V_{SHE}$ and corresponds to the potential for the reaction



in solutions containing $0.1M Cl^-$. As a consequence, deposition of copper would be expected at potentials below

$+0.200V_{SHE}$.

A number of researchers have used copper chloride solutions to accelerate dezincification reactions. A recent paper by Falleiro and Pieske indicates that nickel chloride solutions have a similar accelerating effect on dezincification.⁽⁶¹⁾ This suggested that the acceleration of dezincification caused by these solutions could be explained by the free corrosion potentials of brasses immersed in them.

Tests were run in four solutions which had been reported in the literature to produce rapid dezincification. The experimental setup was identical to that used for the potentiostatic tests except that a Keithley Model 602B Electrometer attached to a strip-chart recorder was used to measure the potential of the sample for a period of 24 hours in the solution of interest. All solutions were stirred vigorously.

The results of these tests on both alpha and beta brasses are summarized in Tables 10 and 11. In every case the observed behavior could be explained in terms of the final steady-state potential reached by the sample. In

Table 10
Alpha Brass Free Corrosion Potential Tests

Solution	Final Potential	Dezincification?	Reference Authors
66 g/l HCl +13.4 g/l CuCl ₂	+0.090V _{SHE}	No	Langenegger and Robinson ⁽⁶²⁾
66 g/l HCl +15.8 g/l CuCl	+0.085V _{SHE}	No	Langenegger and Robinson ⁽⁶²⁾
1M H ₂ SO ₄	+0.058V _{SHE}	Yes	Stillwell and Turnipseed ⁽⁵²⁾
30 g/l NaCl +32 g/l NiCl ₂	-0.290V _{SHE}	Yes	Falleiro and Pieske ⁽⁶¹⁾

Table 11
Beta Brass Free Corrosion Potential Tests

Solution	Final Potential	Dezincification?	Reference Authors
66 g/l HCl +13.4 g/l CuCl ₂	+0.050V _{SHE}	Yes	Langenegger and Robinson ⁽⁶²⁾
66 g/l HCl +15.8 g/l CuCl	+0.100V _{SHE}	Yes	Langenegger and Robinson ⁽⁶²⁾
1M H ₂ SO ₄	+0.050V _{SHE}	Yes	Stillwell and Turnipseed ⁽⁵²⁾
30 g/l NaCl +32 g/l NiCl ₂ ·6H ₂ O	+0.100V _{SHE}	Yes	Falleiro and Pieske ⁽⁶¹⁾

all instances this potential was reached within one hour of the start of the test. The two samples which did not dezincify were both alpha brasses which came to potentials of $+0.090V_{SHE}$ and $+0.085V_{SHE}$. This is in the potential range where stirring was shown to prevent deposition of copper on alpha brass specimens.

DISCUSSION

The two main theories which have been proposed for dezincification have often been considered to be mutually exclusive. Authors claiming that they have found supporting evidence for one or the other mechanism have claimed without further justification that the other conclusion was unwarranted.

Evidence has been presented herein which indicates that each (and sometimes both) mechanism can occur. X-ray analysis and electron microprobe data which support a selective-removal explanation of the dealloying process were obtained from some of the same samples which show copper deposits. Figure 15 shows a diffusion zone in alpha brass which had been exposed in hydrochloric acid. Figure 16 is a photograph of this sample and shows the probe trace in the center of the picture. Figure 16 also shows a copper deposit at the top of the picture, thus illustrating that both mechanisms can occur on the same piece of metal. The two samples which produced the x-ray patterns in Figures 9 and 10 also had deposits on the surface and produced electron-microprobe data indicating the existence of diffusion zones.

The diffusion distances in Figures 12 and 13 are small but are still wide enough to represent several tens of thousands of interatomic distances, and thus they can represent significant diffusion distances. Pickering points out that the diffusion interface is not flat but becomes rough, or rippled.^(64,83) Although this irregular interface usually is too small to be seen metallographically in the case of dealloying in aqueous environments,⁽⁹²⁾ the same effect has been noted on samples subjected to liquid-metal corrosion where the perturbations are large enough to be seen metallographically.⁽¹²⁴⁾ This roughening results in a shorter average diffusion path length than would be available with a flat interface. The distances which are detected with the microprobe are thus probably larger than the actual diffusion path and represent the width of this roughened area rather than the length of the diffusion path itself. Nonetheless, the net diffusion zone still is large enough to be observed with confidence using the electron microprobe.

The electrodeposition of copper from solutions having a significant copper ion concentration can be explained by the Nernst equation

$$E = E^0 + \frac{2.3 RT}{n} \log \frac{a_{\text{CuCl}_2^-}}{a_{\text{Cu(ally)}} (a_{\text{Cl}^-})^2} \quad \text{(Eq. 1)}^*$$

which at room temperature becomes

*The sign convention used herein conforms to that used in calculation of Pourbaix diagrams. See Eq. 76, Appendix 8.

$$E = E^0 + \frac{0.0591}{1} \log \frac{a_{\text{CuCl}_2^-}}{a_{\text{Cu(alloy)}} (a_{\text{Cl}^-})^2} \quad (\text{Eq. 2})$$

for the reaction



The terms of this equation can be separated

$$E = E^0 + 0.059 \log a_{\text{CuCl}_2^-} - 0.0591 \log \left\{ a_{\text{Cu(alloy)}} (a_{\text{Cl}^-})^2 \right\}$$

Variations in either the CuCl_2^- or the Cu(alloy) activity will cause a change in the equilibrium potential for the reaction. In other words, increases in the activity of the complex copper ion will shift the equilibrium in the noble direction. The existence of a copper alloy having a higher copper activity than that of the original alloy will lower the potential. Accordingly, copper is expected to be electrodeposited from solutions at a given potential provided the conditions of Eq. 1 are fulfilled. The $\log a_{\text{Cu(alloy)}}$ term varies only slightly for compositions of from 10-100 percent copper.

Equation 3 implies that copper will be deposited from unstirred 0.1M chloride solutions at potentials below +0.200V_{SHE}. Scanning in the active direction from potentials more noble than +0.200V_{SHE} will result in the onset of copper deposition at this potential. Thus copper deposition is to be anticipated from solutions containing copper ions (either as corrosion products or as added ions) at potentials below +0.200V_{SHE} in 0.1M chloride solutions.

The approximate copper and zinc concentrations which were attained in the three cells in which copper deposits were observed on alpha brass are listed in Table 12. The dezincification factors, Z , vary from 3.8 for 50°C to 25 for 75°C. All these values are substantially higher than the values (slightly above unity) reported by Marshakov and coworkers and in this report for the dezincification of alpha brasses.

The fact that stagnant conditions can lead to dezincification is illustrated in Figure 39 where "holidays" in the stop-off lacquer used to coat all but a certain portion of a sample caused dezincification in areas under the holidays while the uncoated area suffered general dissolution. Three explanations are possible:

1. The copper ion concentration may satisfy conditions necessary for deposition according to the Nernst equation.
2. The concentration of copper in localized areas of restricted flow could exceed solubility limits and cause precipitation of copper.
3. The local electrochemical potential of the brass surface at the corrosion interface could have been altered due to localized differences in the electrolyte within the "flow-restricted" area.

Table 12

Approximate Copper and Zinc Concentrations
in Solutions Where Copper Deposits
Were Observed on Alpha Brass

Temperature of cell	Copper (ppm)	Zinc (ppm)
50°C	1,600	2,600
75°C	500	5,500
100°C	5,900	12,200

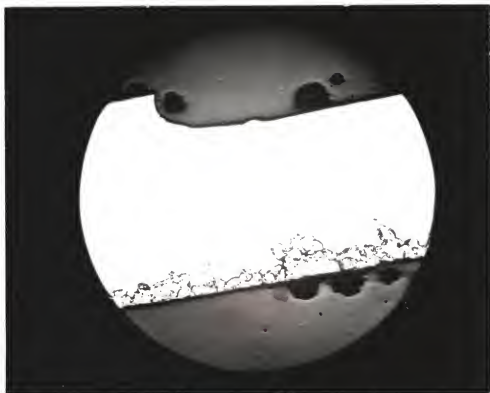


Figure 39. Cross-section of alpha brass showing where holidays in the stop-off lacquer caused dezincification in the stagnant regions beneath the holidays. The unmasked region had no flow restrictions and suffered general dissolution. 25X

The high dezincification factors for beta brass under free-corrosion conditions can be explained as due to the electrochemical potential of beta brass relative to that of alpha brass under conditions where these brasses undergo dissolution. Tanabe⁽¹¹⁰⁾ and Sugawara and Ebiko⁽⁸⁶⁾ report that dealloyed copper alloys quickly become covered with a surface layer of copper which, if the ohmic resistance of the layer is low, presents a copper surface to the bulk solution which is at the free corrosion potential of the alloy. This potential, according to the data of Wilde and Teterin,⁽¹¹³⁾ is lower for beta brass than it is for alpha brass. Thus the potential, or "driving force," difference between the deposition potential of copper from copper chloride solutions (approximately $+0.200V_{SHE}$ for 0.1M chloride solutions) and the potential of the copper surface layer on the brass surface is greater for beta brass than it is for alpha brass.

Sugawara and Ebiko⁽⁸⁶⁾ point out the difficulty of determining the potential of a dealloyed metal at the corrosion interface, which is behind a resistance barrier due to stagnant solution conditions and the presence of the dealloyed layer. Nonetheless, the concept of a Pourbaix diagram for brasses seems to explain experimental observations and provides a basis for predicting conditions under which dealloying is likely to occur.

The Pourbaix diagram approach also explains the effects of stirring on dealloying. LaQue has observed, in salt water

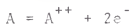
exposure tests of spinning discs of copper alloys, that dealloying (when it occurred) was always observed near the center of the discs where effective water velocity was the lowest.⁽¹²⁵⁾ The outer portions of the same discs were observed to have undergone general corrosion. Although the electrochemical potential was not reported, it is likely that it was in the region indicated by cross-hatching on Figure 36.

Components exposed to conditions involving high relative motion between the part and the electrolyte, such as ship propellers and pump impellers, have also been observed to undergo dealloying. Under these circumstances, it was likely that the potential was in the region indicated by small dots in Figure 36.

Examination of the Nernst equation as written for the dissolution of a divalent metal ion of a hypothetical metal, A,

$$E = E^{\circ} + \frac{2.3 RT}{2} \log a_{A^{++}} - \frac{2.3 RT}{2} \log a_A \quad (\text{Eq. 4})$$

reveals that the term relating to the activity of the copper in the alloy is almost negligible for concentrations of from 10-100 percent A (activities assumed to be proportional to concentration). This is illustrated by a plot of the equilibrium potentials for the equations



and $B = B^{++} + 2e^{-}$

of a hypothetical binary alloy shown in Figure 40. The composition regions in which the activities of the metals in the alloy become significant have been exaggerated so that they can be shown on the graph. There are two regions of interest--the dotted region in the upper left where metal A will not dissolve and element B will, and the larger region where element B will dissolve and element A will not. Both are regions where dealloying is theoretically possible.

This argument would lead to the conclusion that the line on a Pourbaix diagram which separates a region of non-corrosion from a corrosion region would not be displaced radically by alloying. This is contrary to experimental observations made during this study and to the work of others.

The experimental observations of Pickering and Byrne⁽⁹⁸⁾ indicate that copper dissolves from copper-gold alloys at a different potential for copper - 13 percent gold than it does for copper - 18 percent gold. This confirms earlier results⁽⁹⁷⁾ by the same authors on the dissolution of zinc from epsilon, gamma and alpha brasses.

Clearly the Nernst equation cannot explain this aspect of dealloying. The equilibrium potential-pH diagrams for copper and zinc, Figures

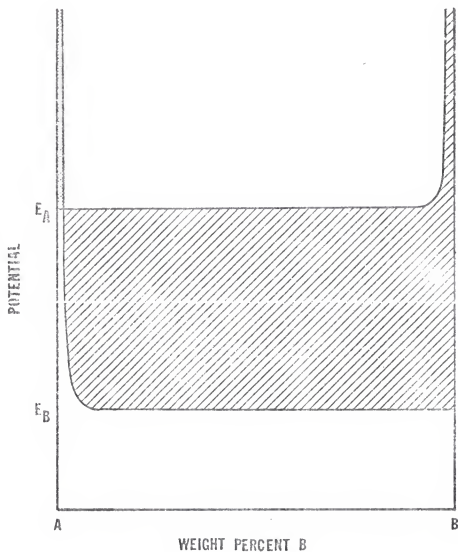


Figure 40. Theoretical domains for dealloying in a given solution based upon the Nernst equation.

34 and 35, were calculated using the Nernst equation for the "immunity" lines. Preliminary investigations into the experimental Pourbaix diagram for pure nickel reveal that there are significant differences between the experimental and theoretical diagrams for nickel. (120,126) The same may hold true for zinc and gold, although the experimental copper diagram in chloride solutions has been determined and agrees closely with many features of the theoretical diagram. (120, 126)

One possibility for the failure of the Nernst equation to explain the experimental observations discussed above is that the calculations were made assuming the activities of the elements in the alloy were directly proportional to the composition. This approximation may not be justified. The activities of constituents of alloys usually are determined at high temperatures and may not be the same at low temperatures. (86,127,128) However, radical departures from ideality are seldom encountered in alloy systems and these departures would have to alter the activities by several orders of magnitude before they would alter the principal points of the above argument.

CONCLUSIONS

On the basis of an analysis of the dezincification of alpha and beta brasses under free corrosion conditions and on the basis of electrochemical behavior of these alloys it may be concluded that:

1. X-ray diffraction and electron microprobe data indicate that a selective-removal process for the dezincification of brasses is operative, at least under certain conditions of potential and pH.

2. Optical evidence and electrochemical evidence indicate that a redeposition mechanism for dezincification can occur under suitable conditions within a particular range of potential and pH.

3. Both operative mechanisms can be observed to have taken place on the same specimen. This can be explained in several ways:

- a) The selective-removal process may actually be one of relative kinetics, i.e., both metals undergo dissolution, but the zinc dissolves much faster, in a certain well-defined range of potential and pH, than copper.

- b) Conditions at the metal-solution interface are altered by the presence of metal ions in solution.

4. Copper enters solution during the dezincification of both alpha and beta brasses under freely corroding conditions (no electrochemical stimulation) in 5N HCl solution.

5. Linear dissolution kinetics were observed for the dissolution of zinc from both alpha and beta brasses for tests ranging up to 120 hours at temperatures up to approximately 100°C.

6. The dissolution kinetics for copper are irregular based on atomic absorption data. This irregularity is believed to be caused at least in part by the morphology of the residual copper layer.

7. The activation energy measured for the dissolution of zinc from beta brass during dezincification was approximately 18 Kcal gm-mole⁻¹. This value is somewhat higher than activation energies for electrochemical dissolution of metals (approximately 10 Kcal gm-mole⁻¹).

8. Because of the seeming irregularity of copper dissolution kinetics it is considered meaningless to calculate an activation energy for copper from atomic absorption data.

9. It is possible to predict domains of potential and pH for each of the operative mechanisms of dezincification by superposition of experimental potential versus pH diagrams over the equilibrium Pourbaix diagrams for the constituent metals of the alloy.

10. The resulting composite diagram provides a basis for understanding the influence of stirring and high flow rates on the dezincification process.

11. The composite diagram also provides an explanation for why tests in copper chloride solutions produce accelerated dezincification.

12. The use of copper chloride solutions to test copper alloys for susceptibility to dealloy is a well-established practice. It is not valid to make conclusions on the mechanism of dezincification based solely on tests in these solutions.

RECOMMENDATIONS FOR FURTHER RESEARCH

The results of this investigation reveal a number of areas of research which should be explored, both for their scientific possibilities and because of their possible economic benefits.

The development of experimental Pourbaix diagrams should be extended to cover all commercial, and potentially commercial, alloy systems. Pourbaix diagrams at elevated temperatures are also needed. Preliminary investigations with single-phase beta brasses reveal that the electrochemical hysteresis technique must be augmented by potentiostatic testing in conjunction with solution analysis investigations.

Identification of in situ reaction products, such as the tarnishes found on potentiostatic samples at low potentials in this study, is an area of importance. Identification of thin films of passive species could lead to important advances in alloy development.⁽¹²⁹⁾ The possibilities of reflectance spectroscopy in the ultraviolet, visible, and infrared spectra should be investigated.

Recent dealuminization failures in aluminum bronzes indicate a need for further understanding of this system of alloys.

C. L. Bulow has suggested that electron microprobe investigations of arsenical duplex alpha-plus-beta brasses might overcome our present lack of understanding and lead to the development of an effective dezincification inhibitor for these alloys. (130)

The irregularities in the copper dissolution data obtained by atomic absorption analysis may well be explained by a systematic study of the evolution of morphology of dealloyed sponges using the scanning electron microscope. The appearance of "annular rings" such as those shown in Figure 17 cannot be explained merely by temperature variations.

"Corrosion tunneling," such as is discussed by P. R. Swann, has a bearing on stress corrosion of some alloys. (131) This is considered to occur by a dealloying mechanism and indicates a further need for morphological studies.

The failure of the Nernst equation to explain dealloying indicates a need for investigations into a reliable method of low-temperature determination of the activities of alloy components.

APPENDICES

APPENDIX 1

EQUIPMENT USED IN ELECTROCHEMICAL TESTS

1. Magna Anatrol Potentiostat Model 4700M with attached Linear-Scan Model 4510.
2. Hewlett-Packard Sanborn Differential Amplifier Model 8875A.
3. Hewlett-Packard Logarithmic Converter Model 7561A.
4. Hewlett-Packard Moseley X-Y Recorder Model 7000A.
5. Corning Calomel Reference Electrode.
6. Keithley Electrometer Model 602B.
7. Beckman pH Meter Expandomatic Model SS-2.
8. Hewlett-Packard Moseley Model 680 Strip Chart Recorder.
9. Duo Seal Vacuum Pump Model 1405H.
10. Acton Model MS64 Electron Microprobe.
11. Cambridge Stereoscan Scanning Electron Microscope with Ortec Energy-Dispersive Si(Li) X-ray Energy Analysis System.
12. Heath Malmstadt Enke Model EU-703-D with Techtron Type AB51 Slot-type Burner.

APPENDIX 2
ELECTROLYTES

pH (± 0.2)	Composition
3.0	0.100 molar NaCl 0.002 molar HCl 0.005 molar $\text{KHC}_8\text{H}_4\text{O}_4$
4.1	0.100 molar NaCl 0.088 molar $\text{KHC}_8\text{H}_4\text{O}_4$ 0.002 molar NaOH
4.5	0.100 molar NaCl 0.016 molar NaOH 0.074 molar $\text{KHC}_8\text{H}_4\text{O}_4$
5.0	0.100 molar NaCl 0.030 molar NaOH 0.060 molar $\text{KHC}_8\text{H}_4\text{O}_4$
5.5	0.100 molar NaCl 0.038 molar NaOH 0.052 molar $\text{KHC}_8\text{H}_4\text{O}_4$
5.9	0.100 molar NaCl 0.042 molar NaOH 0.048 molar $\text{KHC}_8\text{H}_4\text{O}_4$
7.1	0.100 molar NaCl 0.046 molar NaOH 0.045 molar $\text{KHC}_8\text{H}_4\text{O}_4$
8.3	0.100 molar NaCl 0.100 molar NaHCO_3 0.001 molar $\text{KHC}_8\text{H}_4\text{O}_4$
8.6	0.100 molar NaCl 0.100 molar NaHCO_3
9.0	0.100 molar NaCl 0.100 molar NaHCO_3 0.010 molar NaOH

pH (± 0.2)	Composition
9.5	0.100 molar NaCl 0.100 molar NaHCO ₃ 0.020 molar NaOH
10.0	0.100 molar NaCl 0.001 molar NaOH 0.003 molar NaHCO ₃
11.0	0.100 molar NaCl 0.001 molar NaOH
12.0	0.100 molar NaCl 0.010 molar NaOH
13.0	0.100 molar NaCl 0.100 molar NaOH

APPENDIX 3
CHEMICAL ANALYSES OF ALPHA BRASS

Sample Number 6

<u>Element</u>	<u>Weight Percent</u>
Copper	70.47
Lead	0.006
Iron	0.004
Tin	<0.001
Nickel	<0.001
Manganese	<0.002
Silicon	<0.002
Aluminum	<0.001
Tellurium plus Selenium	None detected
Phosphorus	None detected
Bismuth	<0.0005
Zinc	Remainder

Sample Number 55

<u>Element</u>	<u>Weight Percent</u>
Copper	69.82
Lead	<0.006
Iron	<0.004
Tin	<0.001
Nickel	<0.001
Manganese	<0.002
Silicon	<0.002
Aluminum	<0.001
Antimony	<0.01
Phosphorus	None detected
Bismuth	<0.0005
Arsenic	<0.003
Zinc	Remainder

Analyses were supplied by the manufacturer, Chase Brass and Copper Company, Incorporated, who donated the material.

Sample 6 was used for the metallographic, x-ray, electron microprobe, and potentiokinetic studies. Sample 55 was used for atomic absorption and potentiostatic studies.

APPENDIX 4

BETA BRASS INGOT PREPARATION

Beta brass alloys were prepared from 99.99 w/o pure copper and pure zinc stock purchased from the American Smelting and Refining Company. The procedure which follows is similar to that described by Marshakov and coworkers.⁽⁴⁴⁾

Pieces of copper and zinc were cleaned in concentrated HNO_3 followed by rinsing in 1/1 $\text{HNO}_3\text{-H}_2\text{O}$, in distilled water, and finally in acetone after which they were dried under a hot-air blower.

Charges weighing approximately 150 grams were placed in 19 mm O.D. Vycor* vials which then were evacuated and sealed.

The encapsulated charges were placed in a standard heat-treating furnace and the temperature of the furnace was brought up to 1000°C , which is approximately 120°C above the liquidus for the alloy (see Figure 5). After the alloys had been molten for at least four hours, the capsules were removed from the furnace and turned end-over-end at least twice in order to stir the liquid. The capsules were then placed back in the furnace and kept at 1000°C for another

*Trade name, Corning Glass Company.

hour. Then the furnace controller was turned down to 850°C and held for four hours at this temperature.

The capsules were then removed from the furnace and broken, and the ingots were quenched under a water tap.

Top and bottom sections were removed from each ingot and analyzed according to the procedure in Appendix 5. Grain size was quite large, and a typical cross-section would have four or five grains visible after polishing.

APPENDIX 5

PROCEDURE FOR THE ELECTROGRAVIMETRIC CHEMICAL ANALYSIS OF BINARY COPPER-ZINC ALLOYS

The following procedure is adapted from the procedures recommended by the American Society for Testing Materials and by G. H. Ayres, Quantitative Chemical Analysis.

1. Use a balance accurate to 10^{-4} gm for all weighings.
2. Place a one-gram sample of the brass to be analyzed in a 250 ml beaker.
3. Add 17 cc distilled H_2O , 5 ml conc H_2SO_4 , and 3 ml conc HNO_3 to the beaker in the order listed. This solution will become hot and initiate dissolution of the brass.
4. Dilute the mixture to 75 ml and stir, using an inert magnetic stirring bar, until the brass is completely dissolved.
5. Dilute to 200 ml.
6. Electrolyze at 1 amp (approximately 2 volts) for 8 hours using a preweighed platinum gauze electrode as the cathode and a platinum wire placed at least 2 cm from the cathode as an anode.
7. Add 20 ml of water to the solution. If no additional copper deposit is apparent at the new solution level after 15 minutes, assume the electrodeposition is complete.

If copper appears continue electrolysis until no new copper appears when liquid level is raised.

8. Remove cathode from the water with the current still on. Rinse the cathode using distilled water from a wash bottle as the cathode is removed.

9. Rinse the cathode with distilled water and acetone using wash bottles.

10. Dry the cathode using a hot-air blower.

11. Weigh the cathode.

12. The weight percentage of copper in the test sample is given by:

$$\text{w/o Cu} = \frac{\text{weight gain of cathode}}{\text{original weight of sample}} \times 100.$$

13. Zinc content is calculated to be the remainder of the sample.

APPENDIX 6

ANALYSIS OF BETA BRASS INGOTS
USED IN THIS INVESTIGATION

Ingot number	Analysis ^a (w/o)		Investigations in which ingot was used
	Cu	Zn	
23	53.10	46.90	Electron microprobe
36	52.15	47.85	X-ray diffraction, electron microprobe
38	52.56	47.44	Free corrosion potential
44	52.22	47.68	Atomic absorption
45	51.91	48.09	Potentiostatic
56	51.80	48.20	Potentiostatic
58	53.37	46.63	Potentiostatic

^aAll analyses were performed using the procedure described in Appendix 5.

APPENDIX 7

ELECTROCHEMICAL SAMPLE PREPARATION

All samples were sliced into discs on a cut-off wheel and ground at 120 grit on a belt sander. Samples were then hand polished on 240, 320, 480 and 600 grit silicon carbide paper, washed in distilled water, and dried under a hot-air blower.

APPENDIX 8

EQUATIONS USED IN CONSTRUCTION OF POTENTIAL VERSUS pH DIAGRAM FOR THE Cu-Cl-H₂O SYSTEM AND THE Zn-H₂O SYSTEM

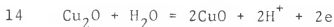
Cu-Cl-H₂O System [extracted from Van Muylder, deZoubov
and Pourbaix⁽¹²⁵⁾]

Eq. #



a) $E = 0.471 - 0.0591 \text{ pH}$ (no hydrated oxides)

b) $E = 0.572 - 0.0591 \text{ pH}$ (assumes hydrated Cu₂O)



a) $E = 0.669 - 0.0591 \text{ pH}$

b) $E = 0.568 - 0.0591 \text{ pH}$ (assumed hydrated Cu₂O
but non-hydrated CuO)

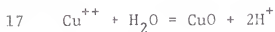


a) $E = 1.648 - 0.0591 \text{ pH}$

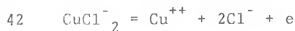
*Equation numbers refer to circled numbers on diagrams,
Figures 34, 35 and 36.

Cu-Cl-H₂O System (continued)

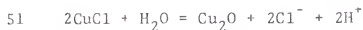
Eq. #



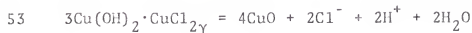
$$a) \quad \log(\text{Cu}^{++}) = 7.89 - 2\text{pH}$$



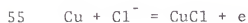
$$a) \quad E = 0.465 = 0.0591 \log \frac{(\text{Cu}^{++})}{(\text{CuCl}_2^-)} \\ + 0.1182 \log(\text{Cl}^-)$$



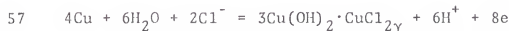
$$a) \quad \log(\text{Cl}^-) = -5.66 + \text{pH}$$



$$a) \quad \log(\text{Cl}^-) = 7.40 + \text{pH}$$



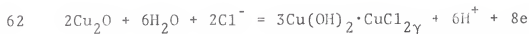
$$a) \quad E = 0.137 - 0.0591 \log(\text{Cl}^-)$$



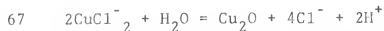
$$a) \quad E = 0.461 - 0.0443 \text{ pH} - 0.0148 \log(\text{Cl}^-)$$

Cu-Cl-H₂O System (continued)Eq. #

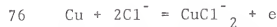
$$\text{a) } E = 0.785 - 0.0886 \text{ pH} + 0.0295 \log(\text{Cl}^-)$$



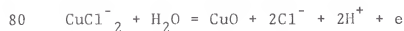
$$\text{a) } E = 0.498 - 0.0148 \log(\text{Cl}^-) - 0.0443 \text{ pH}$$



$$\text{a) } \log(\text{CuCl}_2^-) = 4.45 - \text{pH} + 2 \log(\text{Cl}^-)$$



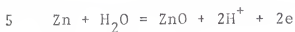
$$\begin{aligned} \text{a) } E &= 0.208 + 0.0591 \log(\text{CuCl}_2^-) \\ &\quad - 0.1182 \log(\text{Cl}^-) \end{aligned}$$



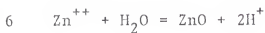
$$\begin{aligned} \text{a) } E &= 0.932 - 0.1182 \text{ pH} - 0.059 \log(\text{CuCl}_2^-) \\ &\quad + 0.1182 \log(\text{Cl}^-) \end{aligned}$$



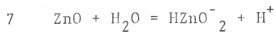
$$\text{a) } E = 0.537 + 0.0591 \log(\text{Cu}^{++}) + 0.0591 \log(\text{Cl}^-)$$

Zn-H₂O System [extracted from Zoubov and Pourbaix⁽¹²⁰⁾]Eq. #

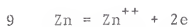
$$a) \quad E = -0.439 - 0.0591 \text{ pH}$$



$$a) \quad \log(\text{Zn}^{++}) = 10.96 - 2 \text{ pH}$$



$$a) \quad \log(\text{HZnO}_2^-) = -16.68 + \text{pH}$$



$$a) \quad E = -0.763 + 0.0295 \log(\text{Zn}^{++})$$

BIBLIOGRAPHY

1. R. Heidersbach, Corrosion, 24, 38 (1968).
2. D. B. Bird and K. L. Moore, Materials Protection, 1, 70 (1962).
3. J. T. Crenell and L. J. E. Sawyer, Journal of Applied Chemistry, 12, 170 (1962).
4. A. F. Blumer, Corrosion, 5, 144 (1949).
5. M. Matsuda, Journal of the Japanese Institute of Metals, 26, 124 (1962).
6. R. B. Niederberger, Modern Castings, 45, 115 (1964).
7. E. P. Polushkin and M. Shuldener, Transactions AIME, 161, 214 (1945).
8. A. L. Simmons, Metal Progress, 57, 496 (1950).
9. A. W. Tracy, ASTM STP, 175, 67 (1956).
10. S. J. van der Baan, Corrosion, 6, 14 (1950).
11. W. H. J. Vernon, Transactions of the Faraday Society, 23, 170 (1927).
12. R. A. Wilkins, Mechanical Engineering, 58 [12], 57 (1936).
13. J. L. Henderson and C. L. Roadhouse, Journal of Dairy Science, 23, 215 (1940).
14. W. C. Stewart and F. L. LaQue, Corrosion, 8, 259 (1952).
15. F. Taylor and J. W. Wood, Engineering, 149, 58 (1940).
16. S. C. Britton, Journal of the Institute of Metals, 67, 119 (1941).
17. L. W. Gleekman and R. K. Swandby, Corrosion, 17, 144t (1961).

18. S. C. Hamstead, Industrial and Engineering Chemistry, 50 [10], 87A (1958).
19. A. H. Hesse, E. T. Myskocoski and B. M. Loring, Transactions of the American Foundrymen's Association, 51, 821 (1944).
20. B. F. Peters, J. A. H. Carson and R. D. Barer, Materials Protection, 4 [5], 24 (1965).
21. M. Schussler and D. S. Napolitan, Corrosion, 12, 107t (1956).
22. J. Serre and J. Lawreys, Corrosion Science, 2, 135 (1965).
23. W. D. Clark, Journal of the Institute of Metals, 73, 263 (1947).
24. P. Trautzel and W. D. Treadwell, Helvitia Chemica Acta, 34, 1723 (1951).
25. L. M. Leedon, Journal of the American Water Works Association, 38, 1392 (1946).
26. A. Dvorak, Strojirentsvi, 12 [1], 39 (1962), referenced by Corrosion Abstracts, 2, 11 (1963).
27. M. G. Fontana, Industrial and Engineering Chemistry, 39 [5], 87A (1947).
28. W. Lynes, Proceedings ASTM, 41, 859 (1941).
29. R. B. Abrams, Transactions of the American Electrochemical Society, 42, 39 (1922).
30. C. F. Nixon, Transactions of the American Electrochemical Society, 45, 297 (1924).
31. J. H. Hollomon and J. Wulff, Transactions AIME, 147, 297 (1942).
32. D. B. Thompson, Australasian Engineering, p. 48 (October, 1954).
33. A. R. Zender and C. L. Bulow, Heating, Piping and Air Conditioning, 16, 273 (1944).
34. E. S. Dixon, ASTM Bulletin No. 102, p. 21 (1940).
35. F. H. Rhodes and J. T. Carty, Industrial and Engineering Chemistry, 17, 909 (1925).

36. J. C. Scully, The Fundamentals of Corrosion, Pergamon Press, New York, 1966.
37. H. H. Uhlig, The Corrosion Handbook, John Wiley and Sons, New York, 1948.
38. K. Hashimoto, W. Ogawa and S. Shimodaira, Journal of the Japanese Institute of Metals, 4 [1], 42 (1963).
39. R. M. Horton, Corrosion, 26 [7], 160 (1970).
40. V. F. Lucey, British Corrosion Journal, 1, 7 (1965); ibid., 2, 53 (1965).
41. L. E. Tabor, Transactions of the Water Works Association, 48 [3], 239 (1963).
42. S. S. Gastev, Izvest. Akad. Nauk. SSR. Metally, 3 (1965), referenced in Corrosion Abstracts, 6, 446 (1966).
43. J. M. Bialosky, Corrosion and Metal Protection, 4, 15 (1947).
44. K. K. Marshakov, V. P. Bogdanov and S. M. Aleikina, Russian Journal of Physical Chemistry, 38 [7], 960 (1964); ibid., 38 [8], 104 (1964); ibid., 39 [6], 804 (1965).
45. W. H. Bassett, Chemical and Metallurgical Engineering, 27, 340 (1922).
46. J. O'M. Bockris, Private communication.
47. B. T. Rubin, PhD Dissertation, University of Pennsylvania, 1969.
48. L. Piatti and R. Grauer, Werkstoffe und Korrosion, 14 [7], 551 (1963).
49. G. T. Colegate, Metal Industry, 73 [507], 531 (1948).
50. L. Kenworthy and W. G. O'Driscoll, Corrosion Technology, 2, 247 (1955).
51. U. R. Evans, The Corrosion and Oxidation of Metals, Edward Arnold and Company, London, 1946.
52. C. W. Stillwell and E. S. Turnipseed, Industrial and Engineering Chemistry, 26, 740 (1934).
53. E. D. Verink, Jr., and P. A. Parrish, Corrosion, 26, 5 (1970).

54. F. W. Fink, Transactions of the Electrochemical Society, 75, 441 (1939).
55. M. N. Desai, J. D. Talati and A. M. Trivedi, Journal of the Indian Chemical Society, 38, 565 (1961).
56. L. Piatti and R. Grauer, Werkstoffe und Korrosion, 14, 551 (1963).
57. M. C. Steele, Australasian Corrosion Engineering, p. 13 (January, 1963).
58. E. D. Verink, Jr., and R. Heidersbach, Jr., "Evaluation of the Tendency for Dealloying in Metal Systems," accepted for publication in an ASTM Special Technical Publication on Localized Corrosion.
59. R. B. Abrams, Transactions of the American Electrochemical Society, 42, 39 (1922); discussion by G. D. Bengough and R. May.
60. C. L. Bulow, in Corrosion Handbook, H. H. Uhlig, editor, John Wiley and Sons, New York, 1948.
61. I. G. S. Falleiro and A. Pieske, Metallurgia, 26 [146], 21 (January, 1970).
62. E. E. Langenegger and F. P. A. Robinson, Corrosion, 24, 411 (1968); ibid., 25, 59 (1969).
63. H. W. Pickering and C. Wagner, Journal of the Electrochemical Society, 114, 698 (1967).
64. H. W. Pickering, Proceedings of the Conference on the Fundamentals of Stress Corrosion Cracking, Columbus, Ohio (1967), NACE, R. W. Staehle, editor, 1969, p. 159.
65. F. P. A. Robinson and M. Shalit, Corrosion Technology, 11 (April, 1964).
66. NACE Standard TM-01-69, "Laboratory Testing of Metals for the Process Industries," published as an insert to Materials Protection, 8 [5] (May, 1969).
67. International Critical Tables of Numerical Data, National Academy of Sciences, Maple Press, York, Pennsylvania, 1929.
68. W. J. Muller, H. Freissler and E. Plettinger, Zeitschrift fur Elektrochemie, 42, 366 (1936).
69. G. D. Bengough and R. May, Journal of the Institute of Metals, 32, 81 (1924).

70. E. D. Verink, Jr., "Construction of Pourbaix Diagrams for Alloy Systems with Special Application to the Binary Fe-Cr System," Report to the Advanced Research Projects Agency, June 10, 1970.
71. P. A. Parrish, MS Thesis, University of Florida, 1970.
72. R. L. Cusamano, MS Thesis, University of Florida, 1971.
73. E. D. Verink, Jr., and M. Pourbaix, "Use of Electrochemical Techniques in Developing Alloys for Saline Exposures," accepted for publication in Corrosion.
74. W. D. France, Jr., and R. W. Liety, "Improved Data Recording for Automatic Potentiodynamic Polarization Measurements," Research Publication GMR-762, General Motors Corp., May 3, 1968.
75. Recommended Practice for a Standard Method for Making Potentiostatic and Potentiodynamic Polarization Measurements, Task Group 2, Potentiostatic and Potentiodynamic Polarization, Section I, Subcommittee XI, ASTM Committee G 1, April 10, 1968.
76. J. E. Reinoehl, F. H. Beck and M. G. Fontana, Corrosion, 26, 141 (1970).
77. W. C. Fort III, High Honors Project, University of Florida, 1971.
78. J. I. Fisher and J. Halperin, Journal of the Electrochemical Society, 103, 282 (1956).
79. H. W. Pickering, Journal of the Electrochemical Society, 115, 143 (1968).
80. L. Graf, Metallwirtschaft, 11, 77 (1932); Zeitschrift fur Metallkunde, 46, 275 (1949).
81. K. Hashimoto, T. Goto, W. Suetaka and S. Shimodaira, Transactions of the Japanese Institute of Metals, 6, 107 (1965).
82. R. Kleinberger, H. Okuzumi and P. Perio, Metaux Corrosion Industries, 35, 40 (1960).
83. H. W. Pickering, Journal of the Electrochemical Society, 117, 8 (1970).
84. E. A. Owen and E. W. Roberts, Philosophical Magazine, 27, 294 (1939).

85. R. Heidersbach, Corrosion, 26, 445 (1970).
86. H. Sugawara and H. Ebiko, Corrosion Science, 7, 513 (1967).
87. L. S. Birks, Electron Probe Microanalysis, Interscience Publishers, New York, 1963.
88. H. G. Feller, Corrosion Science, 7, 359 (1968); Zeitschrift fur Metallkunde, 58, 875 (1968).
89. G. M. Ugiansky and G. A. Ellinger, Corrosion, 24, 134 (1968).
90. K. J. Anusavice, PhD Dissertation, University of Florida, 1970.
91. A. J. Forty and P. H. Humble, Proceedings of the Second International Congress on Metallic Corrosion, 1963, p. 80.
92. H. W. Pickering, Private communication.
93. J. W. Colby, "MAGIC--A Computer Program for Quantitative Electron Microprobe Analysis," Bell Telephone Laboratories, Allentown, Pennsylvania, 1967.
94. J. O'M. Bockris and A. Damjanovic, The Mechanism of the Electrodeposition of Metals, Modern Aspects of Electrochemistry Series, No. 3, Butterworths, Washington, 1964.
95. J. Bumbulis and W. F. Graydon, Journal of the Electrochemical Society, 109, 1130 (1962).
96. T. J. Kagetsu and W. F. Graydon, Journal of the Electrochemical Society, 110, 709 (1963).
97. H. W. Pickering and P. J. Byrne, Journal of the Electrochemical Society, 116, 1492 (1969).
98. Ibid., 118, 209 (1971).
99. R. Potzl and K. H. Leiser, Zeitschrift fur Metallkunde, 61, 525-527 (1970).
100. L. H. Jenkin and R. B. Durham, Journal of the Electrochemical Society, 117, 768 (1970).
101. L. L. Lewis, "A Comparison of Atomic Absorption with Some Other Techniques of Chemical Analysis," in Atomic Absorption Spectroscopy, ASTM STP 443, ASTM, Baltimore, Maryland, 1969.

102. J. Halperin, Journal of the Electrochemical Society, 100, 421 (1953).
103. K. J. Vetter, Electrochemical Kinetics, Academic Press, New York, 1967.
104. P. Kofstad, High Temperature Oxidation of Metals, John Wiley and Sons, New York, 1966.
105. H. H. Willard, L. I. Merritt and J. A. Dean, Instrumental Methods of Analysis, Van Nostrand Reinhold Company, New York, 1965.
106. F. Daniels and R. A. Alberty, Physical Chemistry, John Wiley and Sons, New York, 1961.
107. G. Joseph and M. T. Arce, Corrosion Science, 7, 597 (1967).
108. N. Ohtani, Journal of the Japanese Institute of Metals, 30, 729 (1965).
109. S. Sugawara and S. Shimodaira, Journal of the Japanese Institute of Metals, 30, 765 (1966).
110. Z. Tanabe, Corrosion Science, 4, 413 (1964).
111. H. Gerischer and H. Rickert, Zeitschrift fur Metallkunde, 46, 681 (1955).
112. H. W. Pickering, Journal of the Electrochemical Society, 115, 693 (1968).
113. B. Wilde and G. A. Teterin, British Corrosion Journal, 2, 125 (1967).
114. R. M. Latanision and R. W. Staehle, Proceedings of the Conference on the Fundamentals of Stress Corrosion Cracking, Columbus, Ohio (1967), NACE, R. W. Staehle, editor, 1969, p. 214.
115. E. D. Verink, Jr., and P. A. Parrish, Corrosion, 26, 214 (1970).
116. T. J. Lennox, M. H. Peterson and R. E. Groover, Materials Protection and Performance, 10 [8], 31 (1971).
117. D. C. Vreeland and G. T. Bedford, Materials Protection, 9, [8], 31 (1970).
118. W. B. Brooks, Corrosion, 24, 171 (1968).


119. A. H. Taylor, Journal of the Electrochemical Society, 118, 854 (1971).
120. M. Pourbaix, Atlas of Electrochemical Equilibria in Aqueous Solutions, Pergamon Press, New York, 1966.
121. R. W. Staehle, Private communication.
122. K. D. Efrid, MS Thesis, University of Florida, 1970.
123. J. Van Muylder, N. deZoubov and M. Pourbaix, Report No. 101, CELBECOR, July, 1962, Brussels, Belgium.
124. J. D. Harrison and C. Wagner, Acta Metallurgica, 7, 722 (1959).
125. F. L. LaQue, Private communication.
126. E. D. Verink, Jr., Quarterly Report for the Period Ending June 30, 1971, submitted to the Office of Saline Water, U.S. Department of the Interior, by the Engineering Industrial and Experiment Station, University of Florida, Gainesville, Florida.
127. L. S. Darken and R. W. Gurry, Physical Chemistry of Metals, McGraw-Hill, New York, 1953, p. 249.
128. N. Ohtani, Journal of the Japanese Institute of Metals, 30, 729 (1966).
129. R. Covert, Private communication.
130. C. L. Bulow, Private communication.
131. P. R. Swann, Corrosion, 25, 147 (1969).

BIOGRAPHICAL SKETCH

Robert Henry Heidersbach, Jr., was born December 30, 1940, at El Paso, Texas. He attended public schools in Illinois and Colorado and was graduated from the Colorado School of Mines in 1963, with the degree of Metallurgical Engineer. From 1963 to 1967 he served in the Corps of Engineers of the United States Army and was stationed in Germany and Vietnam. In 1967 he entered the University of Florida; he enrolled in the Graduate School in 1968. He received the degree Master of Engineering in December, 1969. He has pursued the degree of Doctor of Philosophy in the Department of Metallurgical and Materials Engineering since that date.

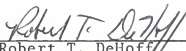
Robert Henry Heidersbach, Jr., is married to the former Dianne Katherine Shrum. He is the father of two children, Robert Scott and Krista Lynn. He is a member of the American Institute of Mining, Metallurgical and Petroleum Engineers, the American Society for Metals, the National Association of Corrosion Engineers, Press Club, and Sigma Alpha Epsilon.

I certify that I have read this study and that in my opinion it conforms to acceptable standards of scholarly presentation and is fully adequate, in scope and quality, as a dissertation for the degree of Doctor of Philosophy.




Ellis D. Verink, Jr., Chairman
Professor of Metallurgical and
Materials Engineering

I certify that I have read this study and that in my opinion it conforms to acceptable standards of scholarly presentation and is fully adequate, in scope and quality, as a dissertation for the degree of Doctor of Philosophy.




Robert T. DeHoff
Professor of Metallurgical and
Materials Engineering

I certify that I have read this study and that in my opinion it conforms to acceptable standards of scholarly presentation and is fully adequate, in scope and quality, as a dissertation for the degree of Doctor of Philosophy.



Robert W. Gould
Associate Professor of
Metallurgical and Materials
Engineering

I certify that I have read this study and that in my opinion it conforms to acceptable standards of scholarly presentation and is fully adequate, in scope and quality, as a dissertation for the degree of Doctor of Philosophy.



John J. Hren
Associate Professor of
Metallurgical and Materials
Engineering

